



**U.S.NRC**

United States Nuclear Regulatory Commission

*Protecting People and the Environment*

NUREG/CR-6977

# **Redox and Sorption Reactions of Iodine and Cesium During Transport Through Aquifer Sediments**

**AVAILABILITY OF REFERENCE MATERIALS  
IN NRC PUBLICATIONS**

**NRC Reference Material**

As of November 1999, you may electronically access NUREG-series publications and other NRC records at NRC's Public Electronic Reading Room at <http://www.nrc.gov/reading-rm.html>. Publicly released records include, to name a few, NUREG-series publications; *Federal Register* notices; applicant, licensee, and vendor documents and correspondence; NRC correspondence and internal memoranda; bulletins and information notices; inspection and investigative reports; licensee event reports; and Commission papers and their attachments.

NRC publications in the NUREG series, NRC regulations, and *Title 10, Energy*, in the Code of *Federal Regulations* may also be purchased from one of these two sources.

1. The Superintendent of Documents  
U.S. Government Printing Office  
Mail Stop SSOP  
Washington, DC 20402-0001  
Internet: bookstore.gpo.gov  
Telephone: 202-512-1800  
Fax: 202-512-2250
2. The National Technical Information Service  
Springfield, VA 22161-0002  
[www.ntis.gov](http://www.ntis.gov)  
1-800-553-6847 or, locally, 703-605-6000

A single copy of each NRC draft report for comment is available free, to the extent of supply, upon written request as follows:

Address: U.S. Nuclear Regulatory Commission  
Office of Administration  
Mail, Distribution and Messenger Team  
Washington, DC 20555-0001

E-mail: [DISTRIBUTION@nrc.gov](mailto:DISTRIBUTION@nrc.gov)  
Facsimile: 301-415-2289

Some publications in the NUREG series that are posted at NRC's Web site address <http://www.nrc.gov/reading-rm/doc-collections/nuregs> are updated periodically and may differ from the last printed version. Although references to material found on a Web site bear the date the material was accessed, the material available on the date cited may subsequently be removed from the site.

**Non-NRC Reference Material**

Documents available from public and special technical libraries include all open literature items, such as books, journal articles, and transactions, *Federal Register* notices, Federal and State legislation, and congressional reports. Such documents as theses, dissertations, foreign reports and translations, and non-NRC conference proceedings may be purchased from their sponsoring organization.

Copies of industry codes and standards used in a substantive manner in the NRC regulatory process are maintained at—

The NRC Technical Library  
Two White Flint North  
11545 Rockville Pike  
Rockville, MD 20852-2738

These standards are available in the library for reference use by the public. Codes and standards are usually copyrighted and may be purchased from the originating organization or, if they are American National Standards, from—

American National Standards Institute  
11 West 42<sup>nd</sup> Street  
New York, NY 10036-8002  
[www.ansi.org](http://www.ansi.org)  
212-642-4900

Legally binding regulatory requirements are stated only in laws; NRC regulations; licenses, including technical specifications; or orders, not in NUREG-series publications. The views expressed in contractor-prepared publications in this series are not necessarily those of the NRC.

The NUREG series comprises (1) technical and administrative reports and books prepared by the staff (NUREG-XXXX) or agency contractors (NUREG/CR-XXXX), (2) proceedings of conferences (NUREG/CP-XXXX), (3) reports resulting from international agreements (NUREG/IA-XXXX), (4) brochures (NUREG/BR-XXXX), and (5) compilations of legal decisions and orders of the Commission and Atomic and Safety Licensing Boards and of Directors' decisions under Section 2.206 of NRC's regulations (NUREG-0750).

**DISCLAIMER:** This report was prepared as an account of work sponsored by an agency of the U.S. Government. Neither the U.S. Government nor any agency thereof, nor any employee, makes any warranty, expressed or implied, or assumes any legal liability or responsibility for any third party's use, or the results of such use, of any information, apparatus, product, or process disclosed in this publication, or represents that its use by such third party would not infringe privately owned rights.

# **Redox and Sorption Reactions of Iodine and Cesium During Transport Through Aquifer Sediments**

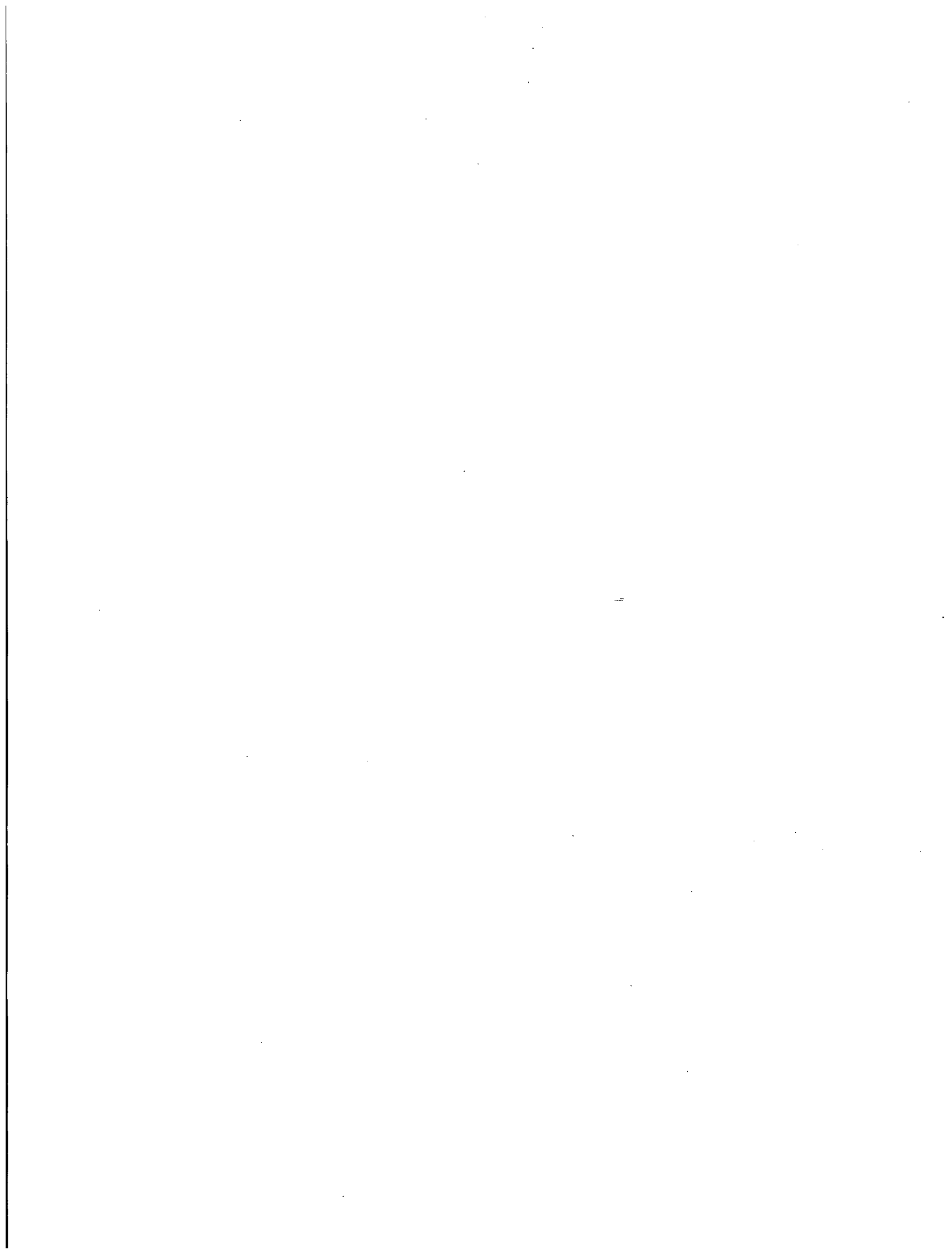
Manuscript Completed: May 2008  
Date Published: March 2009

Prepared by  
J.A. Davis and P.M. Fox

U.S. Geological Survey  
Menlo Park, Ca 94025

M. Fuhrmann, NRC Project Manager

NRC Job Code Y6462



## ABSTRACT

Radioactive isotopes of iodine ( $^{131}\text{I}$  and  $^{129}\text{I}$ ) and cesium ( $^{137}\text{Cs}$ ) are important contaminants present in nuclear waste. These radioisotopes have been introduced into the environment through nuclear weapons tests as well as nuclear accidents such as Chernobyl. Although iodine is commonly found as iodide ( $\text{I}^-$ ), which is generally considered to behave conservatively, it has been proposed that iodide can be oxidized to elemental iodine ( $\text{I}_2$ ) or iodate ( $\text{IO}_3^-$ ) by manganese oxides or nitrate, which may behave less conservatively in sediments due to uptake by organic matter or adsorption onto mineral surfaces. Cesium is generally present as a cation ( $\text{Cs}^+$ ) and can be strongly adsorbed by sediments.

In order to further our understanding of the chemical behavior of I and Cs in groundwater systems, a series of laboratory and field experiments were undertaken. The kinetics of  $\text{I}^-$  oxidation by the manganese oxide, birnessite, was investigated under a variety of geochemical conditions. In order to determine Cs and I sorption and I oxidation, batch experiments with aquifer sediments and with binary sediment-Mn oxide systems were performed. Iodide transport was studied in a column filled with aquifer sediments. Three field tracer test experiments were performed to elucidate the redox chemistry and transport of I and Cs in an aquifer characterized by distinct geochemical zones: (1) injection of  $\text{CsI}$  into a well oxygenated zone of the aquifer, (2) injection of  $\text{CsIO}_3$  into a well oxygenated zone, and (3) injection of  $\text{CsIO}_3$  into a zone of the aquifer characterized by active  $\text{Fe(III)}$  reduction (but not sulfate reduction).

In laboratory experiments, birnessite oxidized  $\text{I}^-$  to  $\text{I}_2$  and  $\text{IO}_3^-$  in a two-step process. The oxidation of  $\text{I}^-$  proceeded according to first order kinetics with respect to initial  $\text{I}^-$  concentration, pH, and birnessite concentration.  $\text{I}_2$  sorption to birnessite was high (up to 0.25 mmol/g), while  $\text{IO}_3^-$  sorption to birnessite was an order of magnitude lower (up to 0.024 mmol/g). Uptake of  $\text{I}^-$  in batch experiments by sediments was fairly low at pH 4.8 or above, as was  $\text{I}^-$  retardation in column experiments at this pH. In column experiments at pH 4.50, the results suggested some oxidation of  $\text{I}^-$  occurred due to a 7% loss of iodine mass exiting the column, presumably due to volatilization of elemental  $\text{I}_2$ .  $\text{IO}_3^-$  uptake in

batch experiments with sediments was higher than that of  $I^-$ , reaching up to 12% adsorbed. Cs also adsorbed to aquifer sediments, with up to 22% removed from solution after 24 hours.

Results from the field tracer tests show that  $I^-$  was oxidized to both  $I_2$  (up to 46%) and  $IO_3^-$  (up to 6%) in the oxic zone, with the extent of oxidation increasing with transport. A pulse of dissolved Mn was liberated from the sediments, providing evidence that Mn oxides were responsible for  $I^-$  oxidation. Iodate was retarded relative to a conservative tracer (Br), arriving 5 days later at 3.9 m downgradient. In the Fe-reducing zone,  $IO_3^-$  was quickly reduced to  $I^-$  without any observed production of  $I_2$  intermediate. About 60% of the iodate was reduced to  $I^-$  in 1 m of transport, with complete reduction occurring after 3 m of transport. Cesium transport was retarded relative to the conservative tracer in all three tracer tests. In the oxic zone of the aquifer, the peak Cs concentration arrived 3.9 m downgradient after 35 days of transport, whereas the Br peak arrived at 8 days. Cs was so attenuated during the first 3.9 m of transport that the maximum Cs concentration reached was only 6% of the injected concentration.

While the Cs and I concentrations used in these experiments was much higher than would be relevant for concentrations of radioactive isotopes of these elements, the studies are relevant for revealing reaction mechanisms that affect the transport of these radionuclides in the environment. The results of these experiments demonstrate that not only can redox transformations of iodine easily occur in groundwater systems, but also that  $I_2$ ,  $IO_3^-$ , and Cs behave non-conservatively by adsorbing to sediments and minerals. The results indicate the importance of considering the complex redox and sorption chemistry of iodine when predicting its transport in waste plumes.

## Foreword

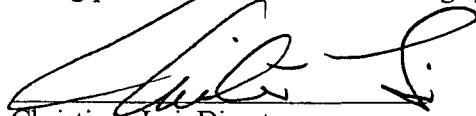
The speciation and related behavior of iodine is controlled by its oxidation state, which can change according to different oxidation/reduction levels found in typical groundwater systems. This report, prepared by staff of the U.S. Geological Survey for the U.S. Nuclear Regulatory Commission, describes experiments examining transport and speciation changes of iodine in groundwater and the rates of speciation change under different levels of oxygen content. These changes substantially affect assumptions about transport of iodine in near surface groundwater and should be considered in Performance Assessment models of systems containing significant quantities of radionuclides of iodine, such as waste forms generated incidental to nuclear fuel reprocessing.

Radioactive isotopes of iodine and cesium are important contaminants with widely differing chemical properties. Cesium is monovalent and tends to strongly adsorb on many minerals. Iodine, in contrast, sorbs poorly and can undergo several oxidation-reduction reactions; the products of these reactions may have differing sorption properties. To further understand the chemical behavior of iodine in groundwater systems, a series of laboratory and field experiments were undertaken. Small-scale batch cesium and iodine sorption experiments were conducted with aquifer sediments and binary sediment-manganese oxide systems. Iodide transport was studied in a column filled with aquifer sediments. Three field tracer experiments were performed to define the redox chemistry and transport of iodine and cesium:

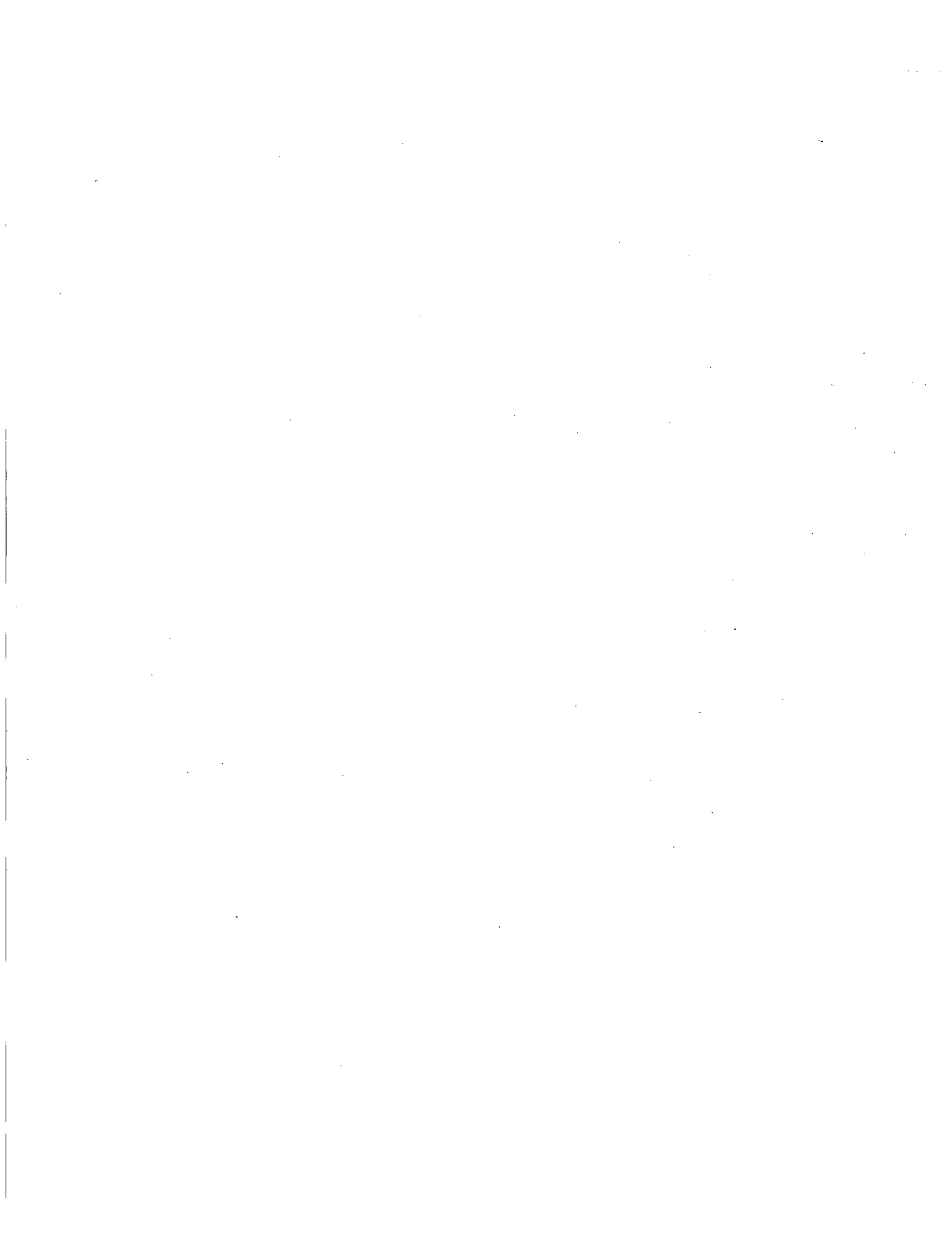
- injection of CsI into a well-oxygenated zone of the aquifer
- injection of CsIO<sub>3</sub> into a well-oxygenated zone of the aquifer
- injection of CsIO<sub>3</sub> into a zone of the aquifer characterized by active iron (III) reduction (but not sulfate reduction).

These experiments were conducted on a very well-characterized, heavily-instrumented site, allowing observation of the differential transport of cesium, iodine, and the conservative tracer bromine.

Redox transformations of iodide easily occurred in oxygenated groundwater systems where it was oxidized to both iodine and iodate. As iodide was oxidized, manganese appeared in the groundwater, indicating that manganese oxides caused the iodine oxidation. In the reducing zone of the aquifer, iodate was reduced to iodide and was transported at the same rate as nonreactive bromine tracer. However, the rate of iodate transport in oxic groundwater was retarded by a factor of about 1.4. In this report, small-scale experiments clarified processes controlling iodine speciation and identified analyses necessary to confirm those processes in the field experiments. The field experiments demonstrated that very small differences in location, associated with changed redox chemistry, can alter iodine speciation and transport and must be considered in conceptual models assessing performance of iodine-bearing systems.



Christiana Lui, Director  
Division of Risk Analysis  
Office of Nuclear Regulatory Research  
U.S. Nuclear Regulatory Commission





## CONTENTS

ABSTRACT .....	iii
FOREWORD.....	v
FIGURES.....	ix
1 INTRODUCTION .....	1
2 LABORATORY STUDIES OF CESIUM AND IODINE ADSORPTION AND REDOX REACTIONS BY AQUIFER SEDIMENTS AND MINERALS .....	3
2.1 Materials and Methods .....	3
2.1.1 Synthesis of Birnessite .....	3
2.1.2 Aquifer Sediments .....	3
2.1.3 Iodine-Birnessite Batch Experiments .....	3
2.1.4 Cesium and Iodine Batch Experiments with Aquifer Sediments .....	4
2.1.5 Column Experiment.....	4
2.1.5.1 Column Packing .....	4
2.1.5.2 Transport Experiment Apparatus.....	4
2.1.5.3 Column Operation .....	5
2.1.6 Iodine and Tritium Analysis .....	5
2.2 Results and Discussion .....	6
2.2.1 Kinetics of Iodide Oxidation by Birnessite .....	6
2.2.1.1 Effect of Ionic Strength .....	6
2.2.1.2 Effect of pH .....	6
2.2.1.3 Effect of Birnessite Concentration .....	6
2.2.1.4 Elemental Iodine Oxidation by Birnessite .....	7
2.2.1.5 Elemental Iodine and Iodate Adsorption .....	8
2.3 Rate Laws and Modeling Predictions .....	8
2.4 Cesium and Iodine Reactions with Aquifer Sediments .....	11
2.4.1 Iodide Adsorption and Oxidation .....	11
2.4.2 Iodate Adsorption .....	12
2.4.3 Cesium Adsorption .....	13
2.4.4 Iodide Transport in Column Experiments with Aquifer Sediments .....	14
2.5 Summary of Laboratory Studies .....	15

3	FIELD STUDIES OF CESIUM AND IODINE TRANSPORT UNDER VARIABLE ENVIRONMENTAL CONDITIONS .....	19
3.1	Site Description .....	19
3.2	Field Experiment Methodology .....	19
3.3	Results and Discussion .....	21
3.3.1	Iodine Oxidation in the Oxidic Iodide Tracer Test .....	21
3.3.2	Iodate Adsorption in Oxidic Iodate Tracer Test .....	21
3.3.3	Iodate Reduction in the Anoxic Iodate Tracer Test .....	22
3.3.4	Cesium Retardation and Attenuation .....	23
3.4	Summary of Field Studies .....	24
4	SUMMARY .....	29
5	REFERENCES .....	31

## FIGURES

Figure 1.1 pe-pH diagram for various redox couples under conditions relevant to the laboratory and field experiments described in this report.....	2
Figure 2.1. Experimental design for column experiment.....	5
Figure 2.2. (A) Iodide oxidation by birnessite (1g/L) at pH 5.00 in 0.1M NaClO <sub>4</sub> solution. The initial I <sup>-</sup> concentration was 1.00 mM. (B) Plot of the same data for the first 8 hours of the experiment.....	7
Figure 2.3 Plot of ln[I <sup>-</sup> ] versus time for 1 mM I <sup>-</sup> oxidation by birnessite (1 g/L) at pH 5.00 in 0.1M NaClO <sub>4</sub> solution.....	7
Figure 2.4. Effect of ionic strength on I <sup>-</sup> oxidation by birnessite at pH 4.5-5.0, showing the disappearance of I <sup>-</sup> and the production of IO <sub>3</sub> <sup>-</sup> and I <sub>2</sub> .....	9
Figure 2.5. Effect of pH on iodide oxidation by birnessite in 0.1M NaClO <sub>4</sub> solution, showing the disappearance of I <sup>-</sup> and production of IO <sub>3</sub> <sup>-</sup> and I <sub>2</sub> .....	9
Figure 2.6. pH dependence of the log of the first order rate constant, k', describing the disappearance of iodide from solution, determined from reacting 1 mM I <sup>-</sup> with 1 g/L birnessite in 0.1M NaClO <sub>4</sub> solution.....	10
Figure 2.7. Oxidation of 0.1 mM I <sup>-</sup> at pH 5.00 in 0.1M NaClO <sub>4</sub> solution for various concentrations of Birnessite, showing the disappearance of I <sup>-</sup> and the production of I <sub>2</sub> and IO <sub>3</sub> <sup>-</sup> versus time.....	10
Figure 2.8. Log-log plot of the pseudo-first order rate constant for iodide disappearance versus birnessite concentration for experiments performed with an initial I <sup>-</sup> concentration of 0.1 mM in 0.1M NaClO <sub>4</sub> solution at pH 5.0.....	11
Figure 2.9. (A) I <sub>2</sub> oxidation by birnessite (1 g/L) at pH 5.00 in 0.1M NaClO <sub>4</sub> solution. The initial iodine concentration was 0.24 mM (as I). (B) Plot of the same data for the first 8 hours of the experiment.....	11
Figure 2.10. Plot of ln[I <sub>2</sub> ] over time for 0.24 mM I <sub>2</sub> (as I) oxidation by birnessite (1 g/L) at pH 5.00 in 0.1M NaClO <sub>4</sub> solution.....	12
Figure 2.11. Log of k' for the disappearance of I <sub>2</sub> from solution determined at 1 g/L birnessite in 0.1M NaClO <sub>4</sub> solution at pH 5.0, plotted against the initial I <sub>2</sub> concentration.....	12
Figure 2.12. Iodine sorption by birnessite (1g/L) at pH 5.0 in 0.1M NaClO <sub>4</sub> solution....	12

Figure 2.13. Iodate sorption by birnessite (1 g/L) at pH 5.0 in 0.1M NaClO <sub>4</sub> solution. (A) Kinetics of IO <sub>3</sub> <sup>-</sup> sorption for sample spiked with 0.50 mM IO <sub>3</sub> <sup>-</sup> . (B) Sorption isotherm showing adsorbed IO <sub>3</sub> <sup>-</sup> versus IO <sub>3</sub> <sup>-</sup> concentration in solution.....	13
Figure 2.14. Comparison of actual (solid lines) and predicted (dashed lines) iodide oxidation by birnessite (1 g/L) using k <sub>1</sub> =1.5 and k <sub>2</sub> =0.0042 for (A) the first 10 hours, and (B) 72 hours.....	13
Figure 2.15. Comparison of actual (solid lines) and predicted (dashed lines) iodide oxidation by birnessite (1 g/L) using k <sub>1</sub> =1.5 and k <sub>2</sub> =0.0473 for (A) the first 10 hours, and (B) 72 hours.....	14
Figure 2.16. Comparison of actual (solid lines) and predicted (dashed lines) iodide oxidation by birnessite (1 g/L) using k <sub>1</sub> =1.5 and k <sub>2</sub> =0.1408.....	14
Figure 2.17. Time dependence of iodide loss from solution via sorption or oxidation by sediments (1000g/L).....	15
Figure 2.18. Time dependence of iodate adsorption onto sediments (400g/L).....	15
Figure 2.19. Iodate adsorption onto sediments (400 g/L) at different pH values after 1 week of reaction.....	16
Figure 2.20. Time dependence of Cs adsorption onto aquifer sediments (400 g/L).....	16
Figure 2.21. Breakthrough curves for tritium ( <sup>3</sup> H) and iodide at pH 4.75 and 4.50.....	16
Figure 3.1. Map of the Cape Cod field site showing the extent of the wastewater plume and the locations of the two study areas (wells F625 and F168).....	20
Figure 3.2. Breakthrough curves showing Br <sup>-</sup> , I <sup>-</sup> , I <sub>2</sub> , IO <sub>3</sub> <sup>-</sup> , and Mn concentrations at various distances downgradient of the injection well in the oxic I <sup>-</sup> tracer test.....	22
Figure 3.3. Iodate and Br breakthrough curves at various distances downgradient from the injection well in the oxic iodate tracer test.....	23
Figure 3.4. Br <sup>-</sup> , IO <sub>3</sub> <sup>-</sup> and I <sup>-</sup> breakthrough curves at various distances downgradient from the injection well for the anoxic iodate injection.....	24
Figure 3.5. Cs, Br, and K breakthrough curves at various distances downgradient from the injection well in the oxic iodide tracer test (well F168-M17-02).....	25
Figure 3.6. Cs, Br, and K breakthrough curves at various distances downgradient from the injection well in oxic iodate tracer test (well F168-M17-08).....	26
Figure 3.7. Cs, Br, and K during the anoxic iodate tracer test (well F625-M12-09).....	27

**TABLES**

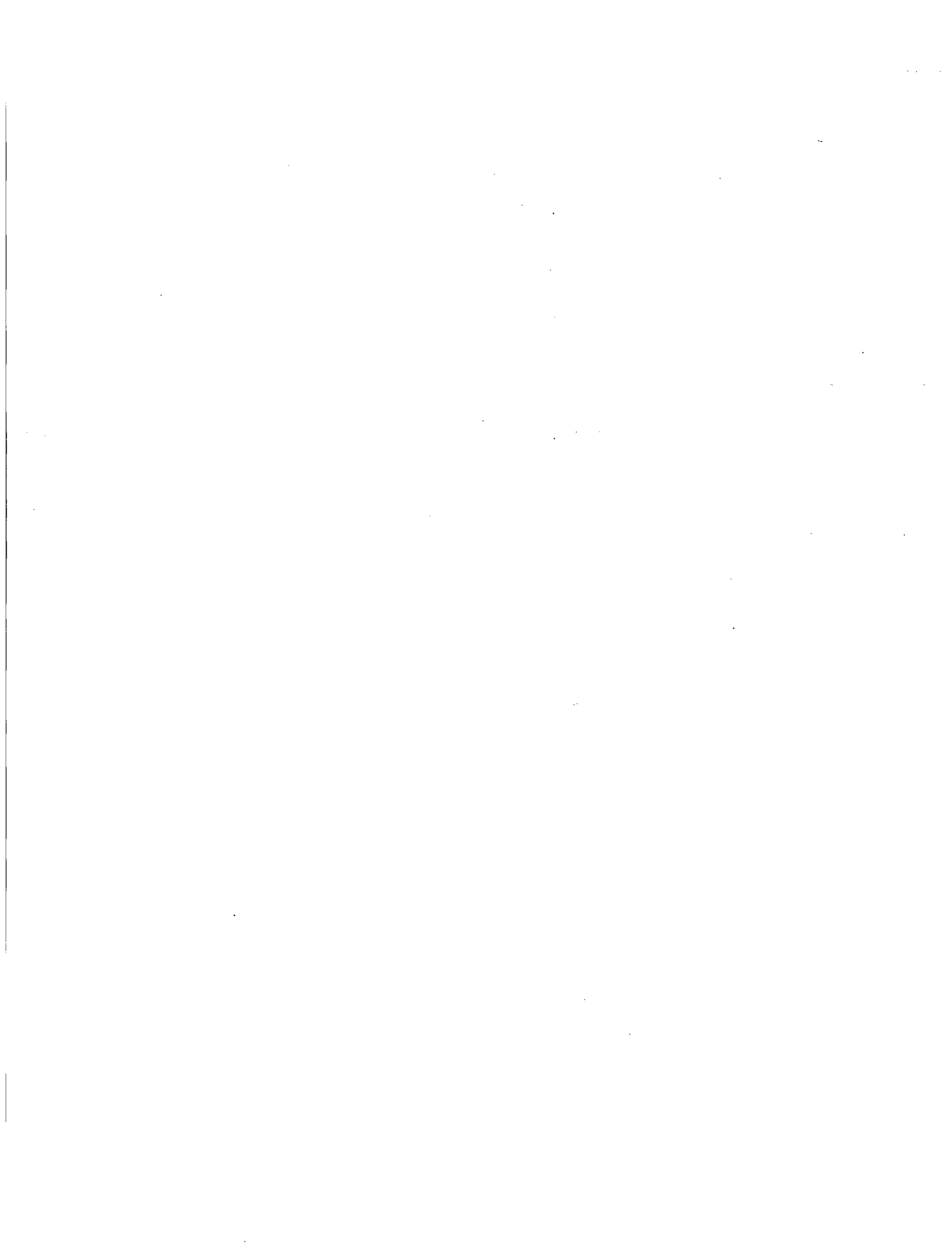
Table 2.1. Basic Characteristics of Aquifer Sediment Composite Samples.....4

Table 2.2. Summary of Pseudo First Order Rate Constants Determined from the Disappearance of The Starting Compound (Iodide Or Iodine).....8

Table 2.3. Reaction Conditions and Speciation of Iodine after Reaction of Iodide with Aquifer Sediments.....15

Table 3.1. Background Chemistry at Injection Wells Used In Field Experiments.....20

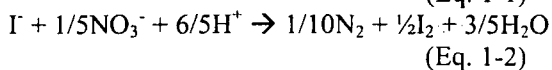
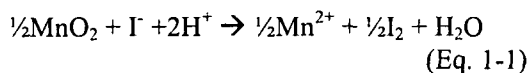
Table 3.2. Tracer Test Characteristics and Injected Tracer Concentrations.....21



# 1 INTRODUCTION

Radioactive isotopes of I and Cs are important contaminants produced from nuclear fission. These radioisotopes are components of nuclear waste and have been introduced into the environment through fallout from nuclear weapons tests and nuclear accidents such as Chernobyl (Filipovic-Vincekovic et al., 1991; Blagoeva and Zikovsky, 1995).  $^{131}\text{I}$  has a very short half life (8 days) and high activity, whereas  $^{129}\text{I}$  has a long half life ( $1.57 \times 10^7$  years). While  $^{129}\text{I}$  is a naturally occurring radioactive isotope of iodine, anthropogenic sources have greatly increased the pool of  $^{129}\text{I}$  in the environment (Rao and Fehn, 1999; Oktay et al., 2000; Reithmeier et al., 2006).  $^{137}\text{Cs}$  and  $^{134}\text{Cs}$  have half lives of 30.2 and 2 years, respectively. An understanding of the chemical behavior of iodine and cesium in natural systems is important for understanding the fate of their radioisotopes derived from nuclear wastes.

Iodine can exist in oxidation states ranging from -1 to +7, but in natural waters is most commonly present as iodide ( $\text{I}^-$ ), iodate ( $\text{IO}_3^-$ ), and organic I (Luther III et al., 1991; Oktay et al., 2001; Schwehr et al., 2005). A pe-pH diagram for various redox couples is shown in Figure 1.1, calculated for conditions relevant to experiments described in this report. While in theory  $\text{O}_2$  may oxidize  $\text{I}^-$ , this reaction is very slow and thus the  $\text{H}_2\text{O}/\text{O}_2$  redox couple is not shown in the diagram. Significant research into the redox behavior of iodine in seawater (e.g. Anschutz et al., 2000; Truesdale et al., 2001) has been performed. Anschutz et al. (2000) proposed manganese oxides ( $\text{MnO}_2$ ) and nitrate as possible electron acceptors in the oxidation of iodide to iodine and/or iodate (see Fig. 1.1):



There is evidence from research in seawater that iodine redox chemistry is linked to that of nitrogen and manganese oxides, however, these reactions have not been directly proven.

Both  $\text{I}^-$  and  $\text{IO}_3^-$  are considered to be highly mobile and unreactive with sediments. Sorption of these species to many minerals and sediments is low (Fuhrmann et al., 1998; Kaplan et al., 2000). While most researchers have found that  $\text{IO}_3^-$  sorption to minerals and sediments is slightly higher than  $\text{I}^-$  sorption (Couture and Seitz, 1983; Hu et al., 2005), the opposite may be true for certain minerals such as magnetite (Fuhrmann et al., 1998). Elemental iodine ( $\text{I}_2$ ) can also be taken up by organic matter, including humic substances (Sheppard et al., 1995; Warner et al., 2000; Schlegel et al., 2006), sorbed to mineral surfaces (Fuhrmann et al., 1998) and volatilized to the atmosphere, providing additional pathways for the non-conservative behavior of iodine.

Cesium is commonly found as the monovalent cation  $\text{Cs}^+$ , and sorbs strongly to sediments via cation exchange (Zachara et al., 2002; Ainsworth et al., 2005). Cs sorption can usually be described using a two site model including a strong site and a weak site corresponding to the frayed edge sites (FES) and planar sites of phyllosilicates, respectively (Poinssot et al., 1999; Zachara et al., 2002). Several researchers have noted that a fraction of the Cs is irreversibly sorbed (Comans et al., 1991; Krumhansl et al., 2001; Zachara et al., 2002).

In this study, a combination of field and laboratory experiments were conducted to further our understanding of Cs and I interactions with aquifer sediments, specifically (1) iodide oxidation, (2) sorption of I species, and (3) sorption of Cs species. Through the use of laboratory experiments, the kinetics of iodide oxidation by the manganese oxide, birnessite, was studied under a variety of conditions, including variable pH, ionic strength, initial I concentration, and solid concentration. Cs and I batch experiments with aquifer sediments and with binary sediment-Mn oxide systems were performed to determine the extent of Cs and I sorption and I oxidation. Iodide transport was also studied in a column filled with natural aquifer sediments.

In addition to laboratory studies, the results of three field experiments are described in the report. Tracer tests were performed to elucidate the redox chemistry and transport of Cs and I in an aquifer characterized by distinct geochemical zones: (1) injection of CsI into a well oxygenated zone of the aquifer, (2) injection of CsIO<sub>3</sub> into a well oxygenated zone, and (3) injection of CsIO<sub>3</sub> into a zone of the aquifer characterized by active Fe(III) reduction (but not sulfate reduction).

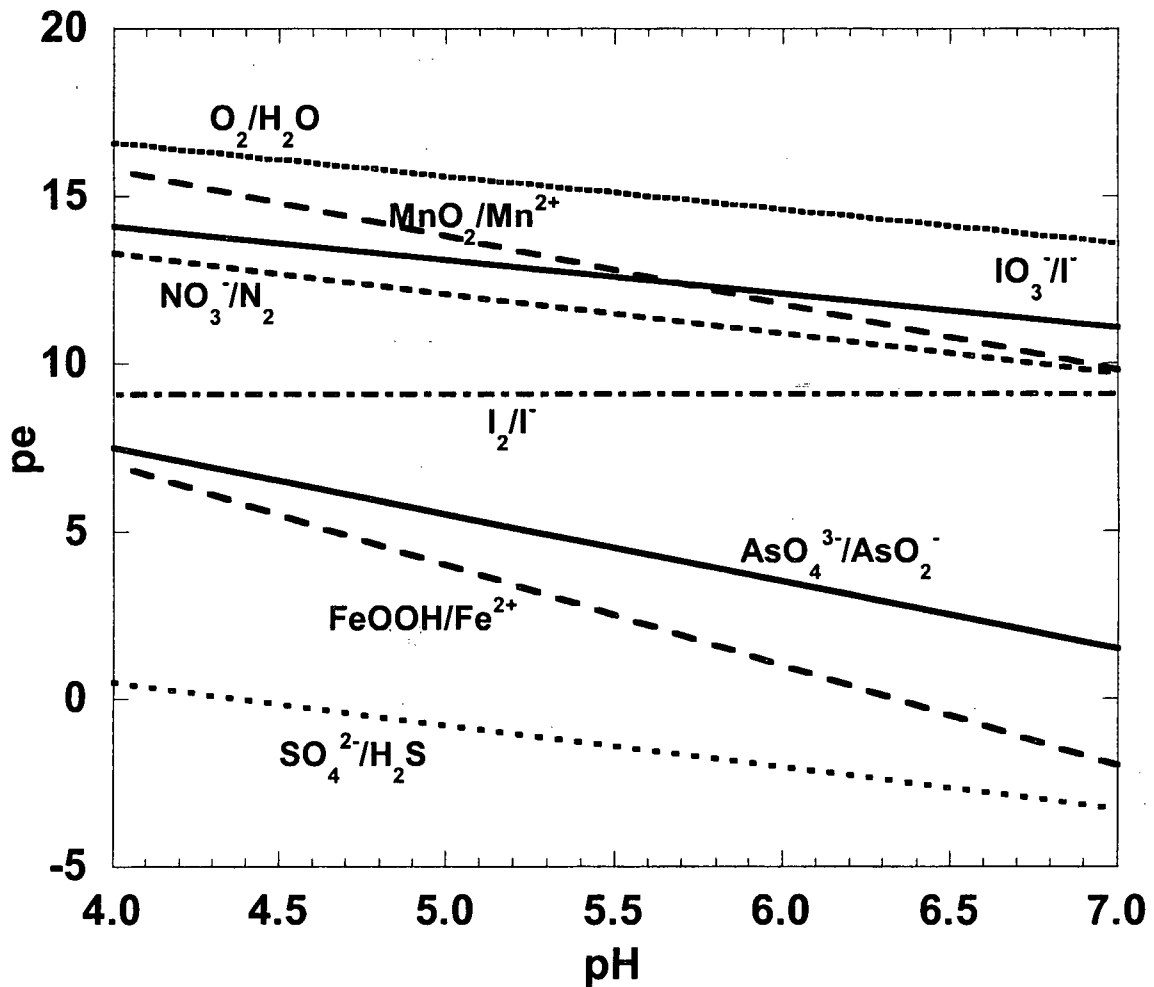


Figure 1.1 pe-pH diagram for various redox couples under conditions relevant to the laboratory and field experiments described in this report. [SO<sub>4</sub><sup>2-</sup>]=10<sup>-4</sup>M; [N<sub>2</sub>]=0.77atm; [O<sub>2</sub>]=0.21atm; [NO<sub>3</sub><sup>-</sup>], [Mn<sup>2+</sup>], [IO<sub>3</sub><sup>-</sup>], [I<sub>2</sub>], [Fe<sup>2+</sup>], [H<sub>2</sub>S]=10<sup>-6</sup>M; and [I<sup>-</sup>]=10<sup>-3</sup>M. The activities for all solid phases and water were taken as 1.0.



## 2 Laboratory Studies of Cesium and Iodine Adsorption and Redox Reactions by Aquifer Sediments and Minerals

### 2.1 Materials and Methods

#### 2.1.1 Synthesis of Birnessite

Birnessite ( $\delta$ - $\text{MnO}_2$ ) was synthesized by adding concentrated HCl to a boiling solution of 0.4M  $\text{KMnO}_4$  (McKenzie, 1971). The resulting precipitate was washed several times with deionized water and then placed in dialysis tubing in a tub of MilliQ-deionized water to further remove salts. The deionized water was changed daily until the conductivity of the rinse water was close to that of MilliQ-deionized water. The solid was confirmed to be birnessite by XRD, and the surface area was determined to be  $41 \text{ m}^2/\text{g}$  by 5 point  $\text{N}_2$ -BET. The average oxidation state of Mn in the solid was determined to be 4.09 by oxalate titration (Hem et al., 1982). The resulting birnessite solid contained 52.4% (w/w) Mn and 9.2% (w/w) K.

#### 2.1.2 Aquifer Sediments

Several sediment composites were used for the batch and column experiments. The composites were created from aquifer materials collected from the oxic zone of a water table in a sand and gravel aquifer located on Cape Cod, Massachusetts. The site where the sediments were collected has been described in detail elsewhere (Davis et al., 2000). The shallow, unconfined aquifer consists of permeable, stratified glacial sand and gravel deposits, with mineralogy dominated by quartz with minor accessory minerals. Surfaces of sediment grains are heavily coated with hydroxypolymer and clay coatings containing Fe, Al and Mn (Coston et al., 1995; Fuller et al., 1996). A description of the collection and characteristics of these sediments is given in Amirbahman et al. (2006) and references therein. One composite sediment sample was collected at the location R23AW, while two other samples were collected near well F168 (F168-15; F168 2005). The sample, F168 2005, was a new composite created to replace the exhausted F168-15 composite.

To prepare composite sample F168 2005, four cores were collected near well F168 and the sediments located 15-20 ft (below ground surface) were air-dried. The sediments were then sieved to remove materials greater than 2mm, and the <2mm fractions from each of the cores were combined to create the composite sample. An aliquot of the new composite was extracted with 0.25M hydroxylamine hydrochloride at  $50^\circ\text{C}$  for 96 hours in order to determine the reductively extractable Mn content. Surface area was measured using 5-point  $\text{N}_2$  BET analysis. The results are compared with the other composites used in this study in Table 2.1. Typical values of extractable Fe(III) can be found in Coston et al. (1995) and Fuller et al. (1996).

#### 2.1.3 Iodine-Birnessite Batch Experiments

Batch kinetic experiments were performed in order to investigate the effect of numerous variables on iodide oxidation by birnessite. Experiments were performed in a gas tight, 4-port 250-mL glass reaction vessel in the dark. Iodide oxidation by birnessite was determined over a range of conditions, including ionic strength (0.01-0.1 M), pH (4.50-6.25), solid-liquid ratio (0.1-1.0 g/L), and initial iodide concentration (0.1-1.0 mM). The kinetics of  $\text{I}_2$  oxidation to  $\text{IO}_3^-$ , and  $\text{IO}_3^-$  adsorption by birnessite were also measured.

The birnessite was suspended in a background electrolyte solution of 0.01 or 0.10 M  $\text{NaClO}_4$  and the pH was adjusted to the desired value with 0.2N HCl or NaOH. The suspension was stirred on a stir plate overnight in order to equilibrate the birnessite prior to iodine addition. The suspension was then spiked with 0.1 M sodium iodide solution, 0.1 M sodium iodate solution, or  $\sim 2 \text{ mM}$   $\text{I}_2$  (as I) stock solution to achieve the desired concentration of I. The  $\text{I}_2$  stock solution was created by shaking several grams of doubly sublimed solid  $\text{I}_2$  in 0.1M  $\text{NaClO}_4$  in the dark for several hours to create a

**Table 2.1. Basic Characteristics of Aquifer Sediment Composite Samples**

<i>Composite</i>	<i>Specific Surface Area</i>	<i>Reductively Extracted Mn</i>
	m <sup>2</sup> /g	μmol/m <sup>2</sup>
R23AW <sup>†</sup>	0.531 ± 0.115	0.59 ± 0.03
F168-15 <sup>†</sup>	0.608 ± 0.074	3.36 ± 0.20
F168 2005	0.764 ± 0.023	1.29 ± 0.05

<sup>†</sup>Data from Amirbahman et al. (2006).

saturated solution, which was filtered and analyzed for I<sub>2</sub> concentration prior to use. The pH of the birnessite suspension was maintained at the target value using a pH stat containing 0.2N HCl throughout the experiment. Samples were periodically withdrawn using a syringe and filtered through a 0.2 μm nylon filter. The first 5 mL of filtered sample were discarded, retaining the next 5-10 mL for analysis. The samples were immediately analyzed for the three iodine species, iodide (I<sup>-</sup>), iodine (I<sub>2</sub>) and iodate (IO<sub>3</sub><sup>-</sup>) by spectrophotometer.

In order to investigate iodate sorption by birnessite, a series of samples were prepared at pH 5.0 in 0.1M NaClO<sub>4</sub> solution with 1 g/L birnessite, and iodate concentrations ranging from 0.005 to 0.500 mM. The batch experiments were performed in duplicate in 35mL polycarbonate centrifuge tubes. The birnessite suspensions were adjusted to pH 5.00 and equilibrated overnight prior to spiking with sodium iodate. Samples were reacted for 22 hours before filtering and analyzing in the same manner as in the kinetic experiments.

#### 2.1.4 Cesium and Iodine Batch Experiments with Aquifer Sediments

Batch experiments were performed in order to investigate the uptake of IO<sub>3</sub><sup>-</sup>, Cs<sup>+</sup>, and I<sup>-</sup> onto the natural sediments from the Cape Cod sand and gravel aquifer. An artificial groundwater (AGW) with a composition designed to match that of the oxic zone of the aquifer was created, containing 0.025 mM CaSO<sub>4</sub>, 0.045 mM MgSO<sub>4</sub>, and 0.25 mM NaCl. In addition, 5 mM MES buffer or 5 mM acetate/acetic acid was added as a pH buffer for experiments performed at pH 5.6 and 4.5-5.2, respectively.

Uptake experiments were performed in polycarbonate centrifuge tubes at a sediment concentration of 400 or 1000 g/L. Sediment samples were mixed with AGW and the pH was adjusted to the target value. Sediments were equilibrated for 24 hours prior to spiking with I<sup>-</sup>, IO<sub>3</sub><sup>-</sup>, or Cs<sup>+</sup> to achieve a final concentration of 1.0 mM (I) or 0.5 mM (Cs). Samples were allowed to react for 2 to 168 hours, then centrifuged and filtered through a 0.45 μm nylon filter and analyzed for iodine species as described below, or Cs by ICP-MS.

Experiments involving sediment amended with synthetic birnessite at rates of 1.0 and 2.7 mg birnessite per g sediment were also conducted as described above.

### 2.1.5 Column Experiment

#### 2.1.5.1 Column Packing

A glass adjustable length column from Millipore (2.2 cm inner diameter, 1 m length) was packed with the F168 2005 composite sediment. The column was packed by suspending the sediment in AGW and pouring the slurry into the column. The excess water was displaced by tightening the adjustable length column plungers. The final packed column length was 98.74 cm at a suspension density of 3849 g/L.

#### 2.1.5.2 Transport Experiment Apparatus

A schematic of the column and pump system is shown in Figure 2.1. It consisted of a stainless steel piston pump (ISCO, 500 mL capacity), two Teflon reservoirs (650 mL), a Teflon tubing (3/16 inch inner diameter) loop, the packed column, an in-line vertical flow pH electrode, and a fraction collector. In order to avoid any

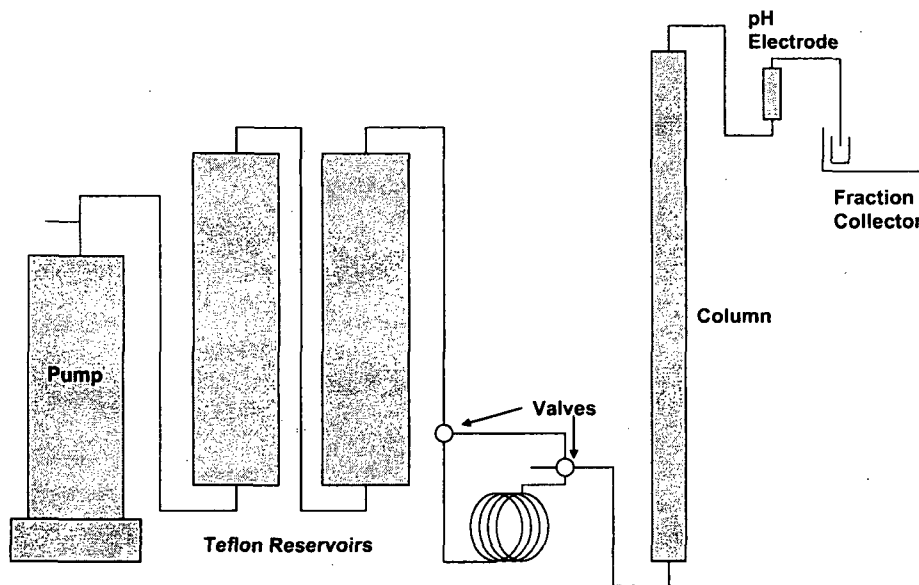


Figure 2.1. Experimental design for column experiment (not to scale).

stainless steel pump, the feed solutions were contained in the Teflon reservoirs (AGW with or without iodide) or the Teflon tubing loop (AGW with tritium), and the pump was filled with a sucrose solution with a density of 1.2 g/mL. The sucrose solution displaced the AGW in the first Teflon reservoir, but was never allowed to reach the second reservoir. All tubing and fittings in the system were Teflon and the valves were 4-way Hamilton valves.

### 2.1.5.3 Column Operation

The flow rate for the duration of the column experiment was 3.17 mL/hr. The column was first preconditioned with AGW at pH 4.75 until the pH of the effluent water stabilized at pH 4.75  $\pm$  0.1 (19 days). Three separate pulses of AGW were pumped through the column: (1) AGW + <sup>3</sup>HHO at pH 4.75, (2) AGW + NaI at pH 4.75, and (3) AGW + NaI at pH 4.50. In between each pulse, AGW was pumped through the column until all traces of the previous pulse were gone from the effluent water. A 5 mM acetate buffer was added to the pH 4.5 AGW in order to help buffer the system at this lower pH. Approximately 2 pore volumes (302.8 mL) of AGW spiked with 10 nCi/mL tritiated water (<sup>3</sup>HHO) was added to the column via the tubing loop. The I<sup>-</sup> pulses (about 3.7 pore volumes

each) were pumped through the column from the Teflon reservoirs. During breakthrough, effluent samples were collected every 0.5 or 1.0 hour. After reaching a plateau, samples were collected every 2 or 3 hours. The tritium pulse was fitted using CXTFIT in order to determine average linear velocity and pore volume of the packed column.

### 2.1.6 Iodine and Tritium Analysis

Iodine species were measured using a UV-Vis spectrophotometer on 3 separate samples: (1) active iodine, (2) active iodine + iodide, and (3) iodate. Active iodine includes elemental I<sub>2</sub> and its hydrolysis products HOI, OI<sup>-</sup>, and in the presence of excess iodide, I<sub>3</sub><sup>-</sup>. For the sake of simplicity, active iodine will be referred to as 'iodine' or 'I<sub>2</sub>' hereafter. Active iodine and iodide (I<sup>-</sup>) were measured using the leuco-crystal violet method (APHA, 1992). Briefly, active iodine (1) is determined by adding a citric acid buffer solution (pH 3.8) to each sample or standard, followed by the addition of the leuco crystal violet indicator solution and measuring absorbance at 592 nm. Active iodine + iodide (2) is determined by the same method with the addition of oxone (KHSO<sub>5</sub>) to oxidize the iodide to iodine. Iodide is then determined by subtraction of (1) from (2). Iodate was

measured by adding an excess of iodide and sulfamic acid and measuring absorbance at 351 nm (Truesdale, 1978). The iodate concentrations were corrected for the presence of  $I_3^-$ . Tritium ( $^3H$ ) was measured by liquid scintillation counting on a Beckman LS 6000 counter.

## 2.2 Results and Discussion

### 2.2.1 Kinetics of Iodide Oxidation by Birnessite

Iodide is oxidized by birnessite to both elemental iodine ( $I_2$ ) and iodate ( $IO_3^-$ ). Figure 2.2 shows speciation data over time for a typical experiment. All of the experiments showed this same general trend, with iodide disappearing fairly quickly followed by a sharp increase in  $I_2$  and a slower production of iodate. It is clear from Figure 2.2 that a significant portion of the iodine is associated with the mineral phase for at least a short period of time. The rates at which these reactions occur vary significantly with factors such as pH and ionic strength. Each of these factors will be discussed further below. The disappearance of iodide over time follows a pseudo first order rate law, and the slope of the plot  $\ln[I^-]$  versus time gives the pseudo first order rate constant ( $k'$ ). An example of this is shown in Figure 2.3, where only the iodide data above the detection limits (the first 2 hours in this case) was used to determine  $k'$ . The pseudo first order rate constants for all experiments are summarized in Table 2.2.

The initial  $I^-$  concentration was varied from 0.1 to 1.0 mM at pH 5.00. The reaction rate did not vary significantly with initial  $I^-$  concentration. For example, with initial  $I^-$  concentrations of 0.1 and 1.0 mM,  $k'$  was determined to be  $1.53 \pm 0.17$  and  $1.39 \pm 0.03$ , respectively. Because the disappearance of  $I^-$  appears to be first order, it is expected that varying the initial  $I^-$  concentration will have no effect on the rate constant.

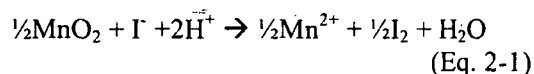
#### 2.2.1.1 Effect of Ionic Strength

Iodide oxidation by birnessite was investigated in 0.01 and 0.10 M  $NaClO_4$  over the pH range 4.50 to 5.00. Increasing the ionic strength slowed down the oxidation reaction (Figure 2.4).

Both the disappearance of  $I^-$  and the production of  $I_2$  and  $IO_3^-$  are slower at higher ionic strength, particularly in the first 2 hours, presumably due to the lower  $I^-$  activity in solution. However, after 8 hours the effect of ionic strength is only apparent in the production of  $IO_3^-$ .

#### 2.2.1.2 Effect of pH

Iodide oxidation by birnessite was investigated for the pH range of 4.50 – 6.50. The loss of  $I^-$  and production of  $I_2$  and  $IO_3^-$  occurs more quickly at lower pH as shown in Figure 2.5. If the log of  $k'$  for each experiment is plotted against pH (Figure 2.6), the slope of the line represents the reaction order with respect to  $H^+$  activity ( $1.02 \pm 0.04$ ). There are two possible explanations for this effect. One involves the pH dependence of iodide oxidation. As seen in equation 2-1, iodide oxidation by birnessite consumes protons, thus it would not be surprising for the rate of oxidation to depend upon the pH.



Acid must be added throughout the experiment in order to maintain a constant pH. However, this trend may also be a reflection of pH dependent adsorption of iodide onto the mineral surface. As the pH drops, the surface charge of the mineral becomes less negative, and the electrostatic repulsion that opposes the specific adsorption of anions decreases. The point of zero charge (pzc) of synthetic birnessite is low (typically around 1.5) and thus the mineral is negatively charged throughout the entire pH range studied (McKenzie, 1981). Several other researchers have demonstrated that  $I^-$  may sorb to sediments and minerals such as illite, ferrihydrite, hematite, and imogolite, and the sorption is often inversely dependent on pH (Couture and Seitz, 1983; Yu et al., 1996; Kaplan et al., 2000).

#### 2.2.1.3 Effect of Birnessite Concentration

The concentration of birnessite was varied from 0.2 to 1.0 g/L in experiments containing 0.1 mM

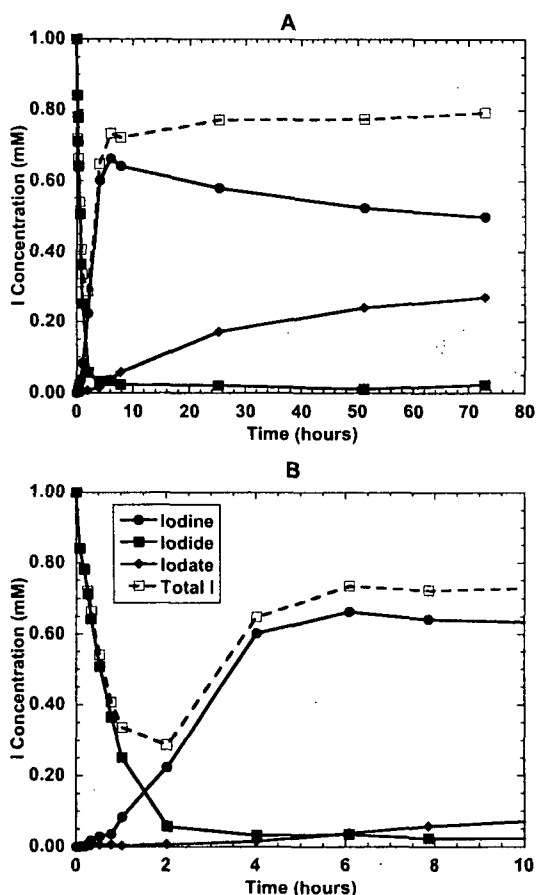


**Figure 2.2. (A) Iodide oxidation by birnessite (1g/L) at pH 5.00 in 0.1M NaClO<sub>4</sub> solution. The initial I<sup>-</sup> concentration was 1.00 mM. (B) Plot of the same data for the first 8 hours of the experiment.**

I<sup>-</sup> (Figure 2.7). In all three cases the available exchange sites on birnessite were in excess of the I<sup>-</sup> concentration. The surface exchange capacity of birnessite (synthesized by the same method used in this study) is reported in the literature to be 25-33  $\mu\text{mol}/\text{m}^2$  (McKenzie, 1981; Scott and Morgan, 1995), corresponding to 1.0-1.4 mmol/g for the birnessite used in this study. The rate of I<sup>-</sup> oxidation was slower at lower birnessite concentrations, for example after 8 hours, 0.010, 0.020, and 0.044 mM of the I<sup>-</sup> had been oxidized to IO<sub>3</sub><sup>-</sup> at 0.2, 0.5 and 1.0 g/L birnessite concentrations, respectively. The log of  $k'$  is plotted against the log of birnessite

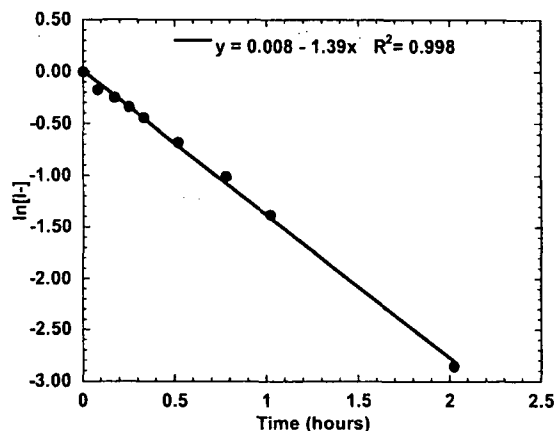


**Figure 2.3 Plot of  $\ln[\text{I}^-]$  versus time for 1 mM I<sup>-</sup> oxidation by birnessite (1 g/L) at pH 5.00 in 0.1M NaClO<sub>4</sub> solution. A linear regression of the data gives a pseudo first order rate constant ( $k'=1.39$ ) for I<sup>-</sup> disappearance (the slope), with the initial I<sup>-</sup> concentration as the intercept.**

concentration in Figure 2.8, with the slope of the line representing the reaction order with respect to birnessite concentration ( $0.98 \pm 0.23$ ). It appears that the reaction is first order with respect to birnessite concentration, however there is a large error associated with this determination because only three data points were used.

#### 2.2.1.4 Elemental Iodine Oxidation by Birnessite

The oxidation of I<sub>2</sub> by birnessite was investigated in order to separate out the two-step oxidation of I<sup>-</sup> to I<sub>2</sub> and I<sub>2</sub> to IO<sub>3</sub><sup>-</sup>. An example is shown in Figure 2.9. There appears to be an initial drop in I<sub>2</sub> concentration which occurs in the first few minutes, which is probably due to adsorption. This is followed by a slower decrease in I<sub>2</sub> concentration and corresponding increase in IO<sub>3</sub><sup>-</sup>. The data from the latter reaction period was used to determine the pseudo first order rate constant ( $k'$ ) for I<sub>2</sub> disappearance (Figure 2.10). Although a plot of  $\ln[\text{I}_2]$  versus time is linear,  $k'$  varied with initial concentration (Table 2.2 and Figure 2.11), indicating that the reaction may not, in fact, follow first order kinetics. The reaction order

**Table 2.2. Summary of Pseudo First Order Rate Constants Determined from the Disappearance of The Starting Compound (Iodide Or Iodine)**

<i>pH</i>	<i>NaClO<sub>4</sub></i> Concentration	<i>Initial I</i> Species	<i>Initial I</i> Concentration	<i>Birnessite</i> Concentration	<i>k'</i> <sup>†</sup> hr <sup>-1</sup>
	M		mM	g/L	
4.50	0.01	I <sup>-</sup>	1.0	1.0	5.30 ± 0.17
4.75	0.01	I <sup>-</sup>	1.0	1.0	1.79 ± 0.06
5.00	0.01	I <sup>-</sup>	1.0	1.0	1.47 ± 0.04
4.50	0.10	I <sup>-</sup>	1.0	1.0	3.25 ± 0.30
4.75	0.10	I <sup>-</sup>	1.0	1.0	2.45 ± 0.06
5.00	0.10	I <sup>-</sup>	1.0	1.0	1.39 ± 0.03
5.25	0.10	I <sup>-</sup>	1.0	1.0	0.627 ± 0.010
5.50	0.10	I <sup>-</sup>	1.0	1.0	0.298 ± 0.013
5.75	0.10	I <sup>-</sup>	1.0	1.0	0.184 ± 0.004
6.00	0.10	I <sup>-</sup>	1.0	1.0	0.118 ± 0.004
6.25	0.10	I <sup>-</sup>	1.0	1.0	0.064 ± 0.003
5.00	0.10	I <sup>-</sup>	0.1	1.0	1.53 ± 0.17
5.00	0.10	I <sup>-</sup>	0.3	1.0	1.57 ± 0.05
5.00	0.10	I <sub>2</sub>	0.31	1.0	0.052 ± 0.002
5.00	0.10	I <sub>2</sub>	0.24	1.0	0.072 ± 0.003
5.00	0.10	I <sub>2</sub>	0.17	1.0	0.089 ± 0.005
5.00	0.10	I <sub>2</sub>	0.05	1.0	0.172 ± 0.009
5.00	0.10	I <sup>-</sup>	0.1	0.2	0.305 ± 0.035
5.00	0.10	I <sup>-</sup>	0.1	0.5	0.552 ± 0.050

<sup>†</sup> *k'* was determined using least squared regression analysis and is expressed along with the standard error.

with respect to initial I<sub>2</sub> concentration was determined to be 0.79±0.07. This indicates that the oxidation of I<sub>2</sub> to IO<sub>3</sub><sup>-</sup> may be more complex than that of I<sup>-</sup> to I<sub>2</sub>; perhaps it is a multistep reaction or is limited by the number of available surface sites on birnessite.

### 2.2.1.5 Elemental Iodine and Iodate Sorption

From Figure 2.9 we can see that when I<sub>2</sub> is added to a suspension of birnessite, there is an initial drop in aqueous I<sub>2</sub> concentration in the first few minutes, followed by a slower decrease that occurs after about 1 hour. We hypothesize here that these two regions represent fast adsorption followed by slower oxidation. The adsorption of I<sub>2</sub> to birnessite was determined by averaging the data points in the 'adsorption' kinetic region. Adsorbed versus aqueous I<sub>2</sub> is plotted in Figure 2.12 below. Although there is

a fair amount of scatter in the data, there is a clear trend especially at lower I<sub>2</sub> concentrations.

Iodate sorption onto birnessite was investigated and found to be rapid, reaching equilibrium within 30 minutes, and fairly low, reaching a maximum of 0.024 mmol/g as shown in Figure 2.13. It is possible that all of the I species adsorb to birnessite, however, other researchers have found IO<sub>3</sub><sup>-</sup> sorption to be greater than I<sup>-</sup> sorption on several minerals and sediments (Couture and Seitz, 1983; Hu et al., 2005). An estimate of the total (sorbed + dissolved) IO<sub>3</sub><sup>-</sup> and I<sub>2</sub> can be calculated from Figures 2.12 and 2.13.

## 2.3 Rate Laws and Modeling Predictions

If we consider the simple case in which oxidation proceeds as a two step reaction from I<sup>-</sup>

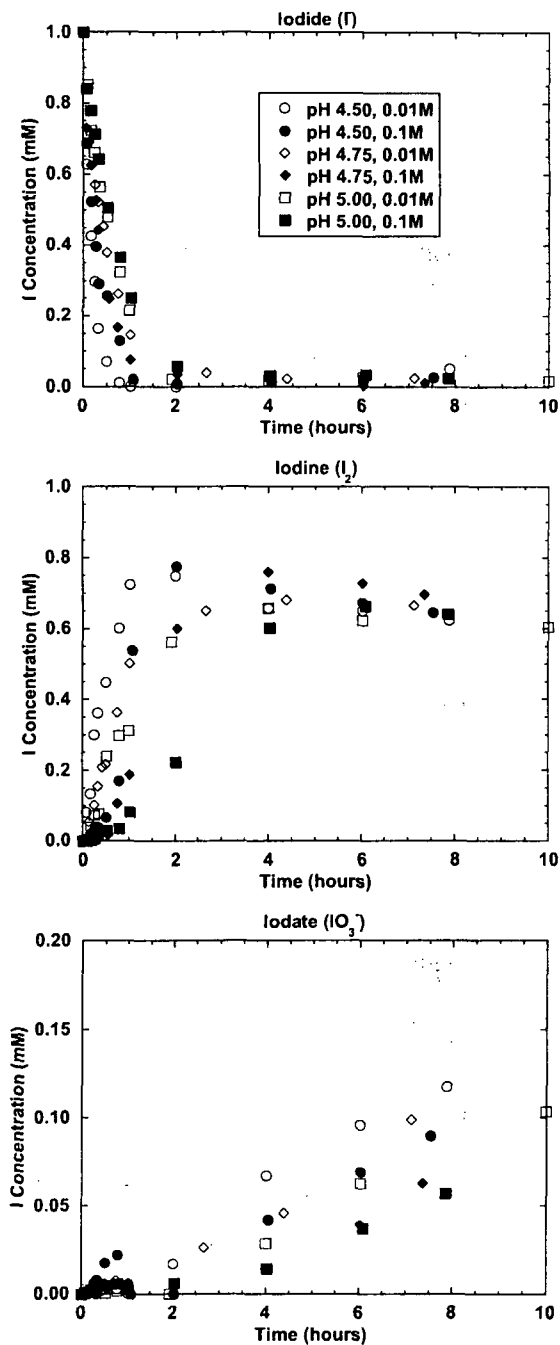


**Figure 2.4. Effect of ionic strength on I<sup>-</sup> oxidation by birnessite at pH 4.5-5.0, showing the disappearance of I<sup>-</sup> and the production of IO<sub>3</sub><sup>-</sup> and I<sub>2</sub>. Suspensions of 1 g/L birnessite were spiked with 1.0 mM NaI solution.**

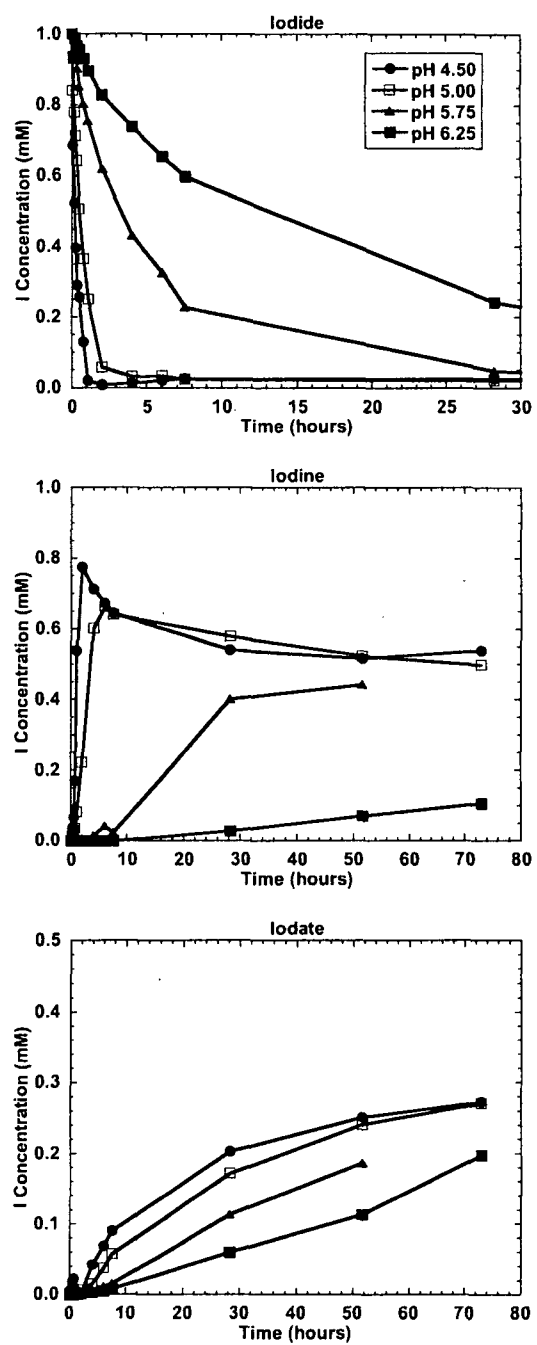


**Figure 2.5. Effect of pH on iodide oxidation by birnessite in 0.1M NaClO<sub>4</sub> solution, showing the disappearance of I<sup>-</sup> and production of IO<sub>3</sub><sup>-</sup> and I<sub>2</sub>. Suspensions of 1 g/L birnessite were spiked with 1.0 mM NaI solution.**

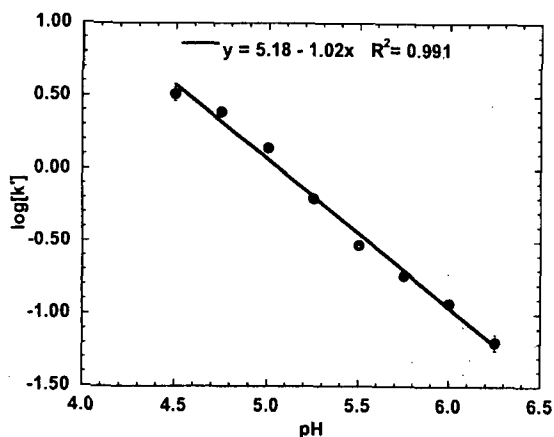


**Figure 2.6. pH dependence of the log of the first order rate constant,  $k'$ , describing the disappearance of iodide from solution, determined from reacting 1 mM  $I^-$  with 1 g/L birnessite in 0.1M  $NaClO_4$  solution. The slope of the line represents the reaction order with respect to hydrogen ion activity.**

to  $I_2$  and then  $I_2$  to  $IO_3^-$  (and both reactions are first order with respect to  $I$ ), then the rate laws can be written as follows:

$$d[I^-]/dt = -k_1[I^-] \quad (\text{Eq. 2-2})$$

$$d[I_2]/dt = k_1[I^-] - k_2[I_2] \quad (\text{Eq. 2-3})$$

$$d[IO_3^-]/dt = k_2[I_2], \quad (\text{Eq. 2-4})$$

where  $k_1$  and  $k_2$  are the pseudo-first order rate constants for the oxidation of  $I^-$  to  $I_2$  and  $I_2$  to  $IO_3^-$  by birnessite, respectively. These equations can be solved for each  $I$  species:

$$[I^-] = [I^-]_0 e^{-k_1 t} \quad (\text{Eq. 2-5})$$

$$[I_2] = [I^-]_0 (k_1 / (k_2 - k_1)) (e^{-k_1 t} - e^{-k_2 t}) \quad (\text{Eq. 2-6})$$

$$[IO_3^-] = [I^-]_0 (1 + ((k_1 e^{-k_2 t} - k_2 e^{-k_1 t}) / (k_2 - k_1))), \quad (\text{Eq. 2-7})$$

where  $[I^-]_0$  is the initial iodide concentration. Under a given set of conditions, e.g. pH 5.00, 1 g/L birnessite in 0.1M  $NaClO_4$  solution, we can determine  $k_1$  from the disappearance of iodide to be 1.5 (average of 3 values). As discussed above, in a given experiment the disappearance of  $I_2$  appears to follow first order kinetics

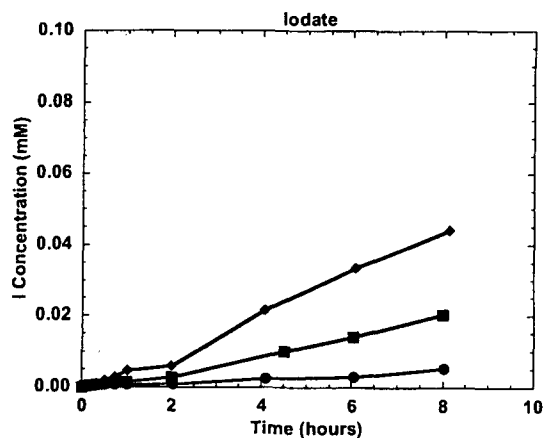
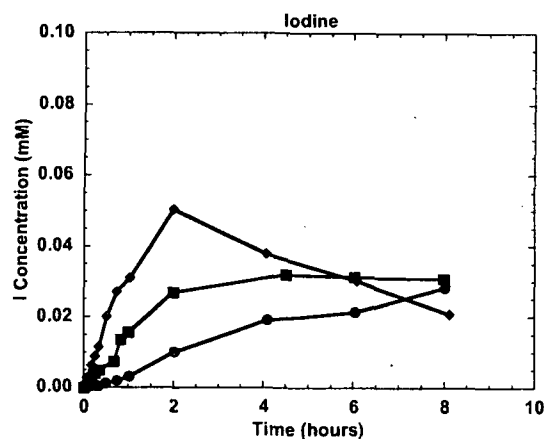
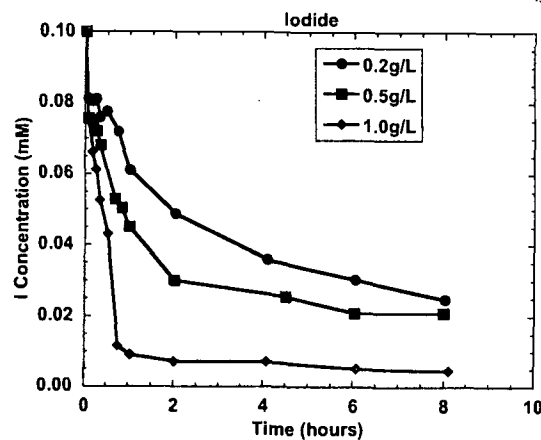


**Figure 2.7. Oxidation of 0.1 mM  $I^-$  at pH 5.00 in 0.1M  $NaClO_4$  solution for various concentrations of Birnessite, showing the disappearance of  $I^-$  and the production of  $I_2$  and  $IO_3^-$  versus time.**



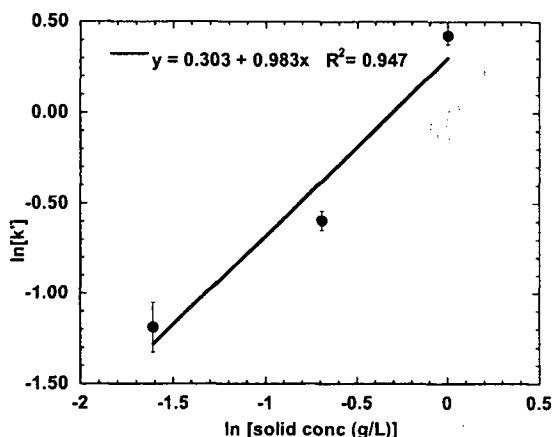


**Figure 2.8.** Log-log plot of the pseudo-first order rate constant for iodide disappearance versus birnessite concentration for experiments performed with an initial  $I^-$  concentration of 0.1 mM in 0.1M  $NaClO_4$  solution at pH 5.0. The slope of the line represents the reaction order with respect to birnessite concentration.

(Figure 2.10). However, the pseudo-first order rate constant ( $k_2$ ) determined from these experiments ranges from 0.052 to 0.173 for initial  $I_2$  concentrations of 0.31 to 0.05 mM indicating that this reaction is complicated by a multi-step reaction or is limited by the available surface sites (Table 2.2 and Figure 2.11). As an approximation, we can treat the oxidation of  $I_2$  to  $IO_3^-$  as a first order reaction by determining  $k_2$  for each individual reaction. Over longer time periods (after all of the  $I^-$  has been oxidized to  $I_2$ ),  $k_2$  can be determined simply from the disappearance of  $I_2$ . Equations 2-5, 2-6, and 2-7 can then be used to predict the concentrations of all three I species over time as shown in Figures 2.14 through 2.16. The model overpredicts the concentration of  $I_2$  during the beginning of the experiment, but predicts the overall shape of the data fairly well. The overprediction of  $I_2$  concentrations may be due to an inaccurate estimate of the amount of sorbed  $I_2$  during this time period or may reflect the presence of sorbed  $I^-$ . If there is significant sorbed  $I^-$  present, then the reaction consists of fast  $I^-$  sorption followed by a slower oxidation to  $I_2$ .

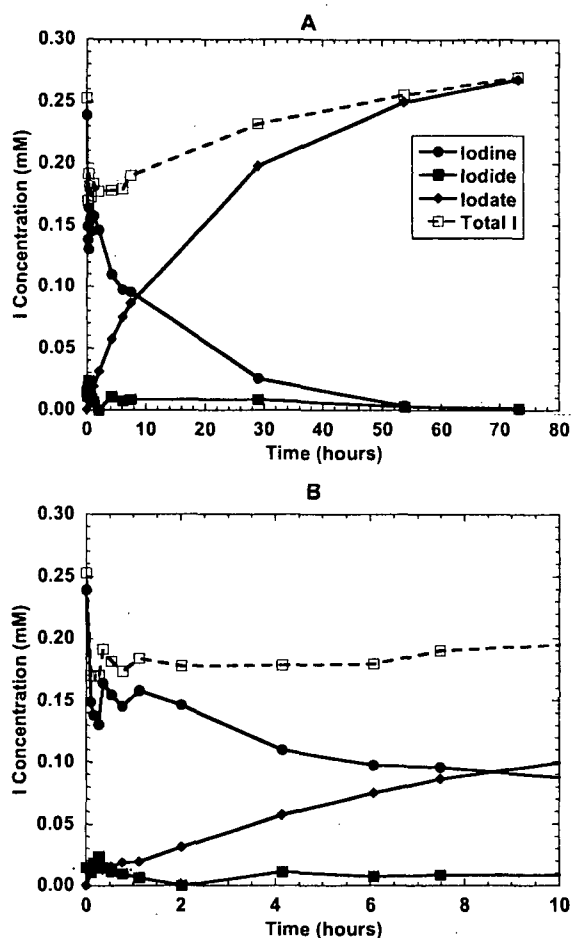


**Figure 2.9.** (A)  $I_2$  oxidation by birnessite (1 g/L) at pH 5.00 in 0.1M  $NaClO_4$  solution. The initial iodine concentration was 0.24 mM (as I). (B) Plot of the same data for the first 8 hours of the experiment.

## 2.4 Cesium and Iodine Reactions with Aquifer Sediments

### 2.4.1 Iodide Adsorption and Oxidation

All sediments were very unreactive with iodide under the conditions investigated (Table 2.3, Figure 2.17). Only under the most favorable conditions for  $I^-$  oxidation, namely lower pH and higher Mn oxide content of F168-15, was there any appreciable uptake of  $I^-$ . In experiments with unamended sediments, oxidized I ( $IO_3^-$  or  $I_2$ )

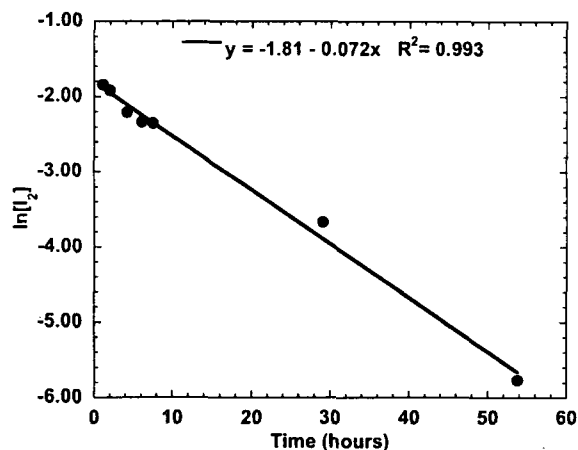


**Figure 2.10.** Plot of  $\ln[I_2]$  over time for 0.24 mM  $I_2$  (as I) oxidation by birnessite (1 g/L) at pH 5.00 in 0.1M  $NaClO_4$  solution. A linear regression of the data gives the pseudo first order rate constant ( $k'=0.072$ ) for  $I_2$  disappearance (the slope), with the initial  $I_2$  concentration as the intercept.

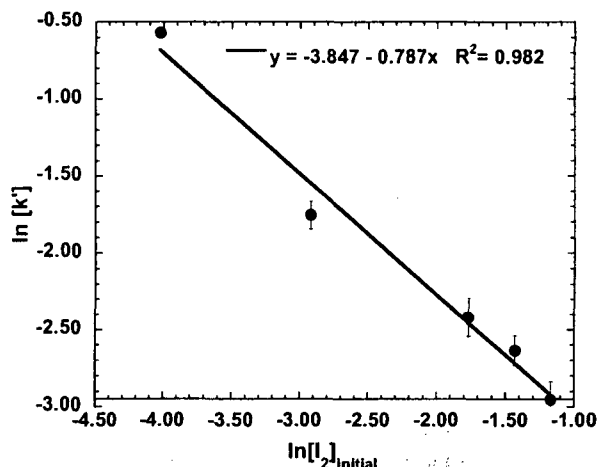


**Figure 2.11.** Log of  $k'$  for the disappearance of  $I_2$  from solution determined at 1 g/L birnessite in 0.1M  $NaClO_4$  solution at pH 5.0, plotted against the log of the initial  $I_2$  concentration. The slope of the line represents the reaction order with respect to the initial  $I_2$  concentration.

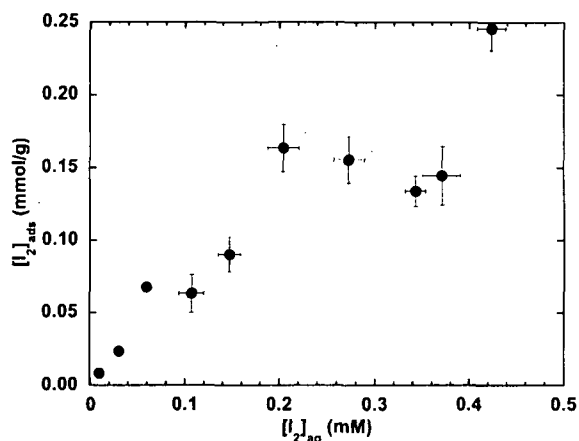


**Figure 2.12.** Iodine sorption by birnessite (1g/L) at pH 5.0 in 0.1M  $NaClO_4$  solution. Several data points in the first 10-30 minutes of  $I_2$  reaction with birnessite were averaged (i.e. before the onset of oxidation to  $IO_3^-$ ). Error bars represent the standard deviation for the averaged values.

was below detection limits in most cases. However, the addition of a Mn oxide (birnessite,  $\delta$ - $MnO_2$ ) to the sediments significantly increased the loss of iodide from solution. It is interesting to note that less than 2% of the total I added to experiments with 1.0 mg/g  $MnO_2$  was detected, however at higher amendment levels of  $MnO_2$  (2.7 mg/g), close to 4 and 5% of the total I was detected as iodate and elemental iodine, respectively. These experiments were not performed in a gas-tight system, so  $I_2$  may be lost to volatilization or taken up by the solid phase, as was observed in experiments with pure birnessite.

## 2.4.2 Iodate Adsorption

As can be seen in Figures 2.18 and 2.19, sediment sample R23AW was fairly unreactive with iodate, with only 2% adsorption at pH 5.7 (initial  $IO_3^-$  concentration = 1.0 mM). However, a relatively slow adsorption of iodate onto F168 sediments occurred, reaching 10-12% for F168-15 sediments after 1 week and 9.2% for F168

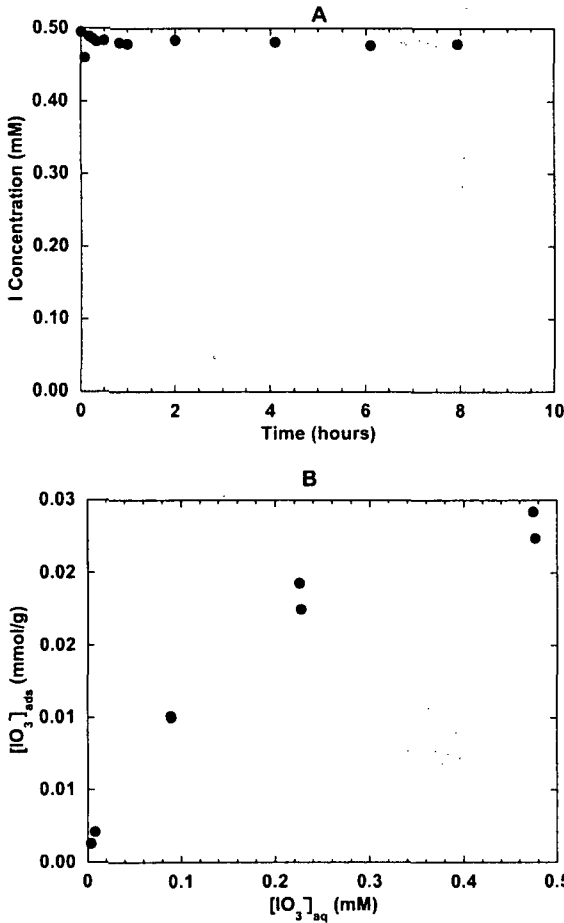


**Figure 2.13. Iodate sorption by birnessite (1 g/L) at pH 5.0 in 0.1M NaClO<sub>4</sub> solution. (A) Kinetics of IO<sub>3</sub><sup>-</sup> sorption for sample spiked with 0.50 mM IO<sub>3</sub><sup>-</sup>. (B) Sorption isotherm showing adsorbed IO<sub>3</sub><sup>-</sup> versus IO<sub>3</sub><sup>-</sup> concentration in solution.**

2005 sediments after 72 hours, perhaps due to the lower pH of these samples. Samples were also analyzed for other iodine species, but none were detected indicating that reduction of iodate was not important in this system. Some other researchers have noted that uptake of IO<sub>3</sub><sup>-</sup> by soils and minerals was due to reduction of IO<sub>3</sub><sup>-</sup> to I<sub>2</sub>, however, these studies involved Fe(II) minerals (pyrite) or anaerobic conditions (Fuhrmann et al., 1998; Yamaguchi et al., 2006).

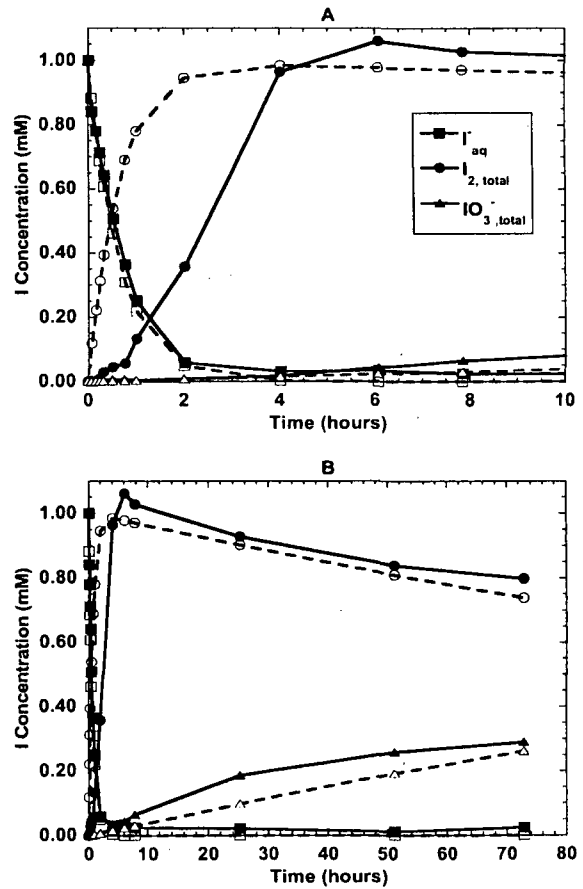


**Figure 2.14. Comparison of actual (solid lines) and predicted (dashed lines) iodide oxidation by birnessite (1 g/L) using  $k_1=1.5$  and  $k_2=0.0042$  for (A) the first 10 hours, and (B) 72 hours.  $[I]_0=1.0$  mM, pH=5.0, and  $[NaClO_4]=0.1$ M. Actual IO<sub>3</sub><sup>-</sup> and I<sub>2</sub> are plotted as total (dissolved + adsorbed) concentration, and I<sup>-</sup> as dissolved only.**

### 2.4.3 Cesium Adsorption

Unsurprisingly, Cs adsorption to aquifer sediments was much more extensive than I adsorption. After approximately 24 hours, 22% and 12% of the Cs was sorbed to sediment samples R23AW and F168 2005, respectively (Figure 2.20). Most of the Cs uptake by the sediments appears to occur quickly (within a few hours), although slight increases in Cs uptake

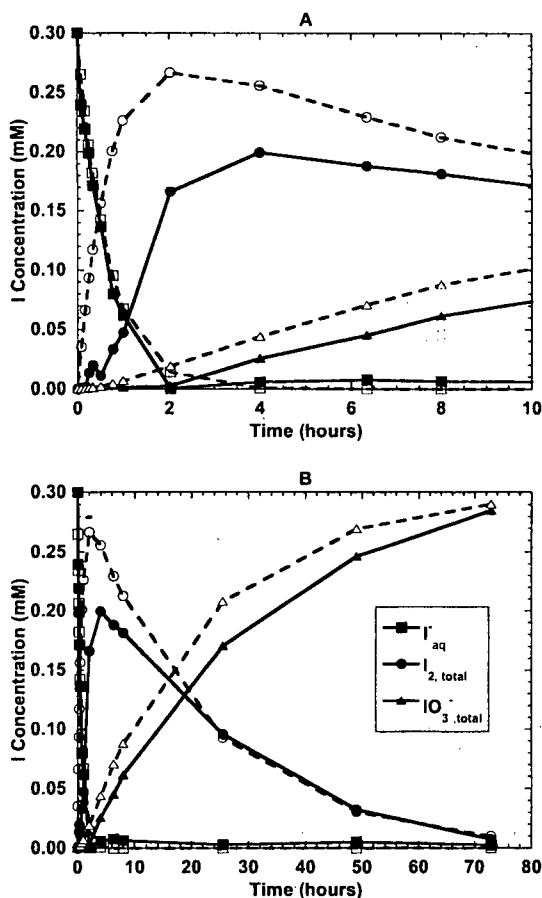


**Figure 2.15.** Comparison of actual (solid lines) and predicted (dashed lines) iodide oxidation by birnessite (1 g/L) using  $k_1=1.5$  and  $k_2=0.0473$  for (A) the first 10 hours, and (B) 72 hours.  $[I^-]_0 = 0.3$  mM, pH=5.0, and  $[NaClO_4]=0.1$ M. Actual  $IO_3^-$  and  $I_2$  are plotted as total (dissolved + adsorbed) concentration, and  $I^-$  as dissolved only.

may continue over longer periods of several days. Other researchers have also observed strong Cs sorption by sediments (Zachara et al., 2002; Ainsworth et al., 2005). Poinssot et al. (1999) noted that Cs sorption to the low affinity, planar sites on illite occurred within a few hours, while sorption onto the high affinity frayed-edge sites took up to 5 days to reach equilibrium. At the high Cs concentrations used in this study, adsorption should be dominated by the low-

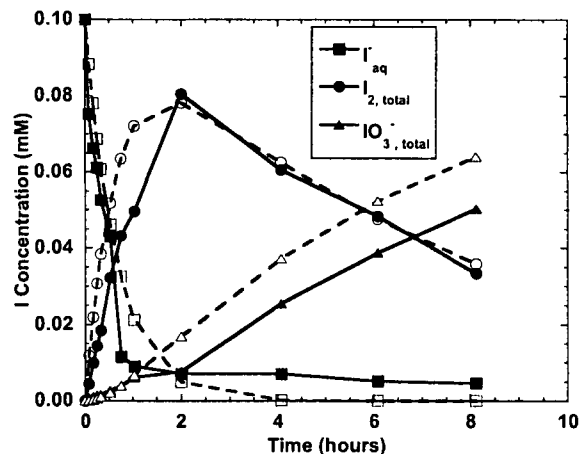


**Figure 2.16.** Comparison of actual (solid lines) and predicted (dashed lines) iodide oxidation by birnessite (1 g/L) using  $k_1=1.5$  and  $k_2=0.1408$ .  $[I^-]_0=0.1$  mM, pH=5.0, and  $[NaClO_4]=0.1$ M solution. Actual  $IO_3^-$  and  $I_2$  are plotted as total (dissolved + adsorbed) concentration, and  $I^-$  as dissolved only.

affinity planar sites. The presence of  $I^-$  had no effect on Cs adsorption (data not shown).

#### 2.4.4 Iodide Transport in Column Experiments with Aquifer Sediments

Figure 2.21 shows breakthrough curves for tritium and iodide in a column packed with the F168 2005 composite sediment sample. The tritium curve was fitted using CXTFIT, and the pore volume was found to be 140.6 mL; the average linear velocity was found to be 0.534 m/day. When iodide was added to the column at pH 4.75, the concentrations increased during breakthrough to about 97% of the input concentration, and then slowly increased to 100% over the next couple of days. There was no indication of iodide retardation during transport, with the breakthrough curve during the first pore volume being virtually identical to that observed for tritium. In the experiment at pH 4.50, however, iodide concentrations increased rapidly to 90% of the inlet concentration, and then reached a maximum of 93% before declining as the pulse of introduced iodine passed. Because no elemental  $I_2$  or iodate

**Table 2.3. Reaction Conditions and Speciation of Iodine after Reaction of 1.0 mM Iodide with Aquifer Sediments**

Sediment	Amendment	Solid conc	Reaction Time	Final pH‡	mM		
					$IO_3^-$	$I_2$	$I^-$
R23AW	mg/g	g/L	hr				
R23AW	None	400	168	5.7	BDL†	BDL	0.993
R23AW	None	400	168	5.1	BDL	BDL	0.976
F168-15	None	400	168	5.1	0.002	0.003	0.979
F168-15	None	400	168	5.0	0.003	0.003	0.927
F168 2005	None	1000	48	4.6	BDL	BDL	0.940
F168 2005	None	1000	24	4.9	BDL	BDL	0.967
F168 2005	1.0 (MnO <sub>2</sub> )	1000	48	5.0	0.002	BDL	0.017
F168 2005	2.7 (MnO <sub>2</sub> )	1000	48	4.9	0.039	0.049	BDL

†BDL= below detection limits of 0.001 mM ( $IO_3^-$ ) and 0.002 mM ( $I_2$ ).

‡ The pH drifted up from the initial values by up to 0.5 pH units. The pH value at the end of the experiment is shown.

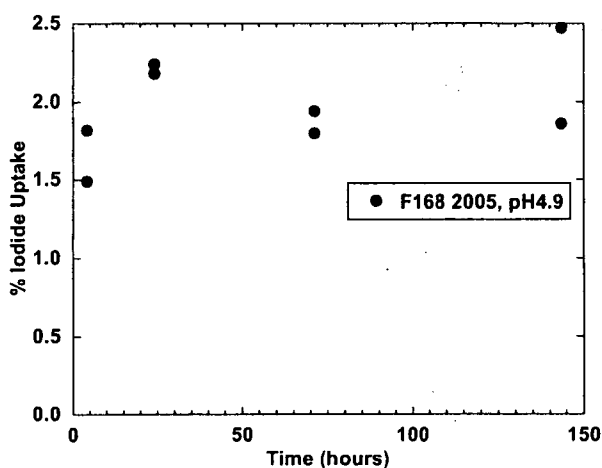


**Figure 2.17. Time dependence of iodide loss from solution via sorption or oxidation by sediments (1000g/L). The initial I concentration was 1.0 mM.**

was detected in the effluent, the results indicate a loss of iodine mass during the experiment. The most likely explanation for the loss is oxidation of iodide to elemental  $I_2$  with subsequent volatilization from samples open to the atmosphere in the effluent fraction collector.

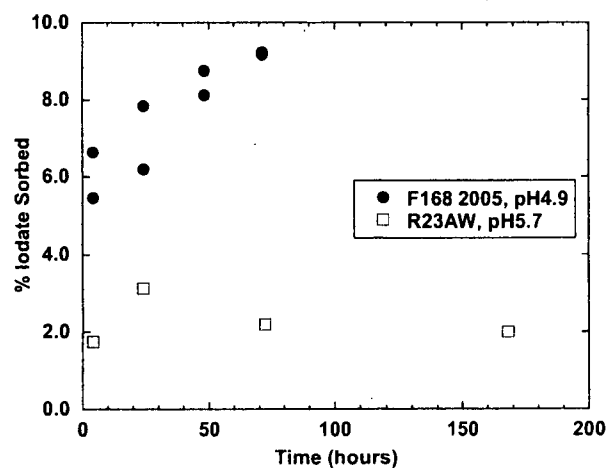


**Figure 2.18. Time dependence of iodate adsorption onto sediments (400g/L). The initial iodate concentration was 1.0 mM.**

## 2.5 Summary of Laboratory Studies

Birnessite, a Mn-oxide mineral commonly present in soils and sediments, was shown to oxidize  $I^-$  to  $I_2$  and  $IO_3^-$  in a two-step process. The oxidation of  $I^-$  proceeded according to first order kinetics with respect to initial  $I^-$  concentration, pH, and birnessite concentration. While  $I_2$  sorption to birnessite was high (up to 0.25 mmol/g),  $IO_3^-$  sorption on birnessite was an order of magnitude lower (up to 0.024 mmol/g). Uptake of  $I^-$  by sediments was near zero in batch

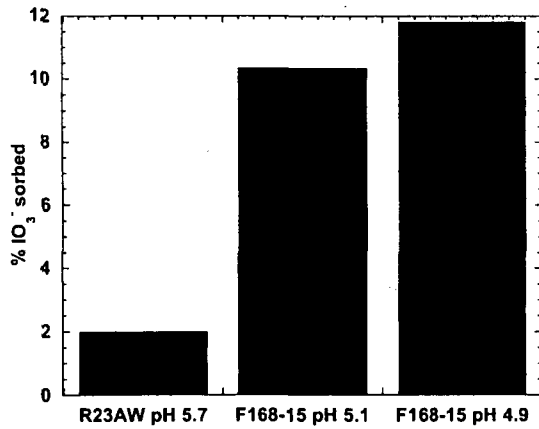


**Figure 2.19. Iodate adsorption onto sediments (400 g/L) at different pH values after 1 week of reaction. The initial iodate concentration was 1.0 mM.**

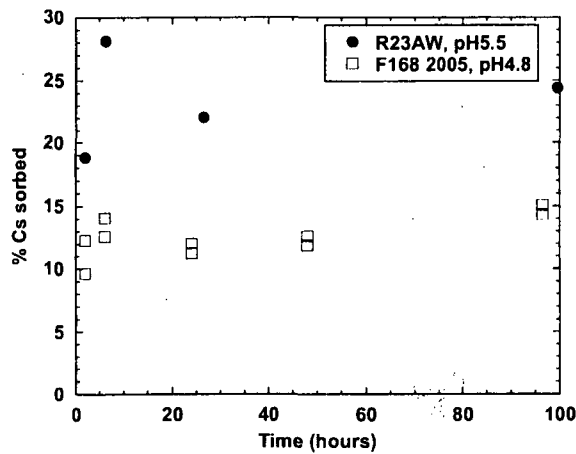


**Figure 2.20. Time dependence of Cs adsorption onto aquifer sediments (400 g/L). The initial Cs concentration was 0.5 mM.**

(<2.5%) and column experiments at pH 4.8 or above, but at pH 4.50, uptake of I<sup>-</sup> in column experiments was significantly higher (I<sup>-</sup> concentrations reached a maximum of 93% of the input concentration). IO<sub>3</sub><sup>-</sup> uptake by sediments was higher than that of I<sup>-</sup>, reaching close to 12% for the F168-15 sediment sample at pH 4.9 (initial I concentration of 1.0 mM). Cs uptake by sediments was higher than that of I<sup>-</sup>, with 22 and 12% sorbed to the R23AW and F168 2005 sediment samples after 24 hours (initial Cs concentration of 0.5 mM).

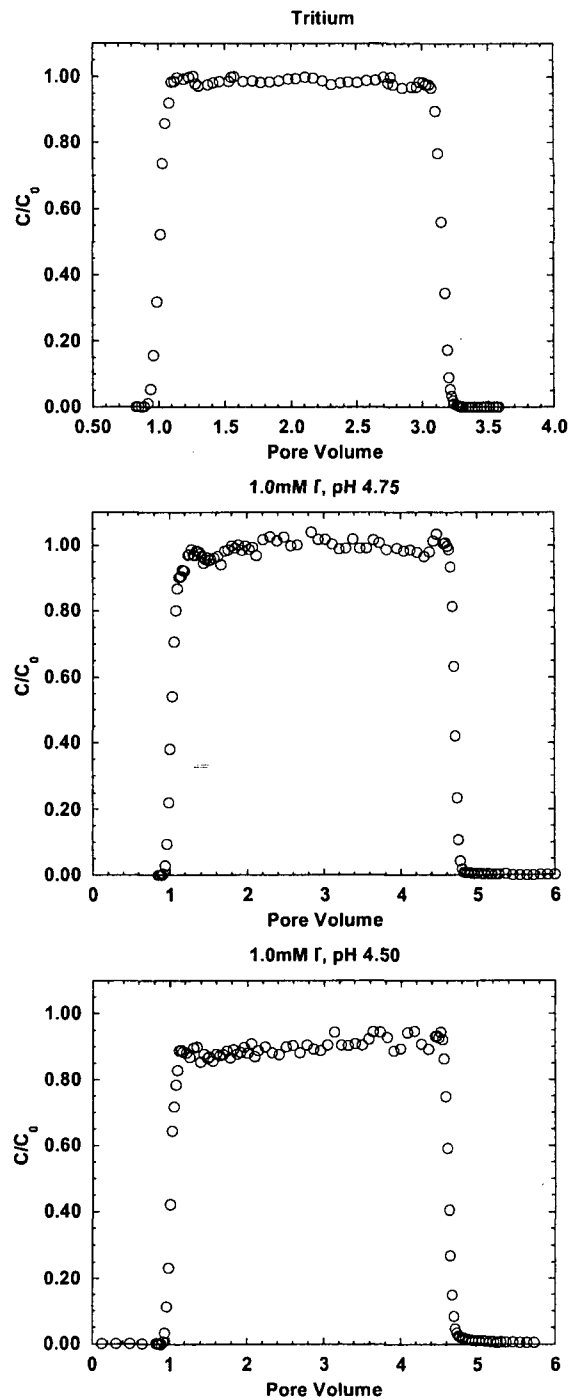
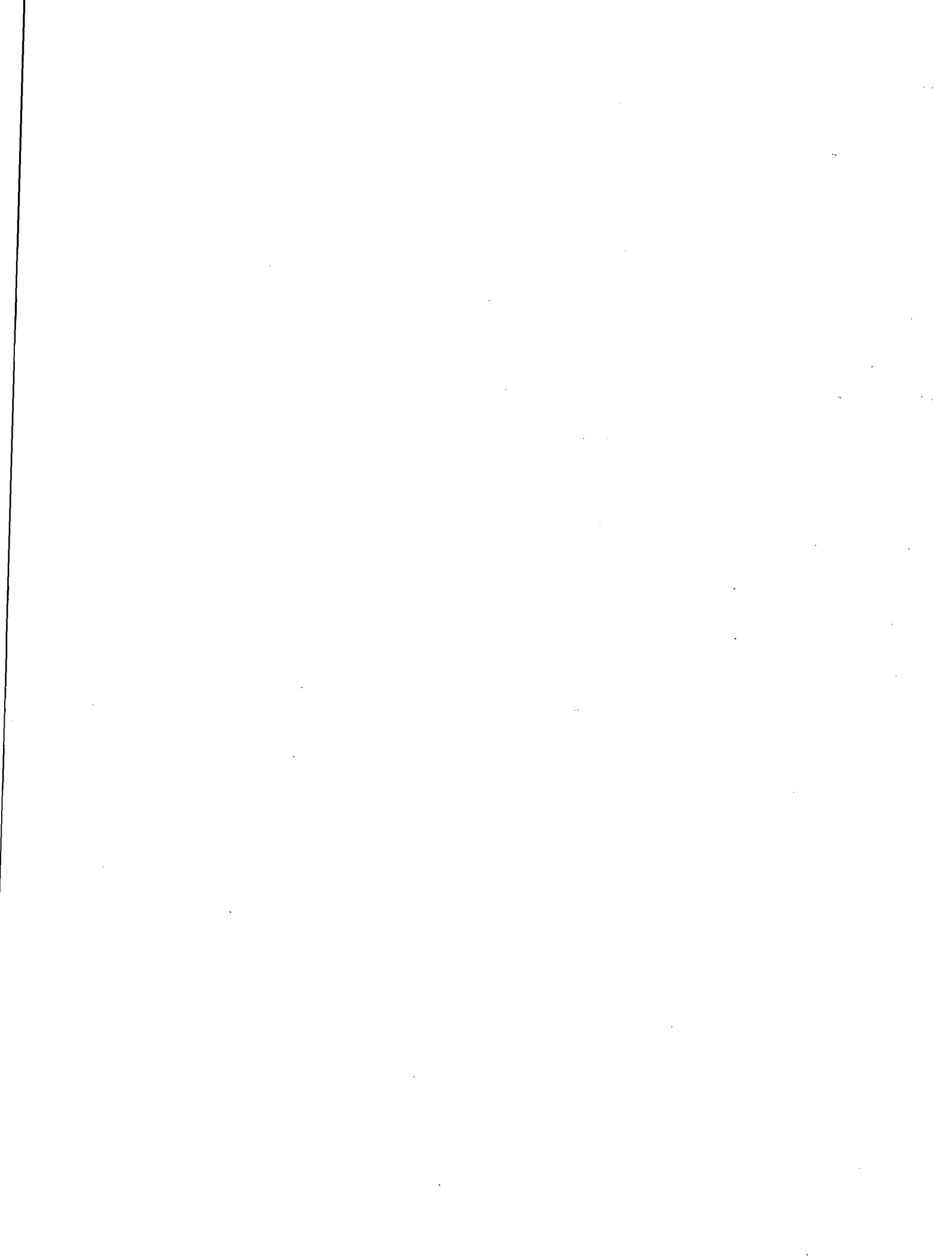


**Figure 2.21. Breakthrough curves for tritium (<sup>3</sup>H) and iodide at pH 4.75 and 4.50. Concentrations are expressed relative to the input concentrations.**

While the Cs and I concentrations used in these experiments are much higher than would be relevant for concentrations of radioactive isotopes of these elements, the studies are relevant for revealing reaction mechanisms that affect the transport of the radionuclides in the environment.





### 3 Field Studies of Cesium and Iodine Transport under Variable Environmental Conditions

#### 3.1 Site Description

Field experiments were performed in a shallow, unconfined sand and gravel aquifer located in western Cape Cod, MA. Discharge of effluent from a sewage treatment plant operated by the Massachusetts Military Reservation from 1938 to 1995 resulted in a plume of sewage-contaminated groundwater characterized by high concentrations of dissolved salts, no dissolved  $O_2$ , higher pH, and the presence of dissolved Fe(II) (Kent et al., 1994). The Fe-reducing sewage contaminated zone is overlain by pristine groundwater characterized by low dissolved salts, high dissolved  $O_2$ , and lower pH. Ground-water flow velocities are approximately 0.4 m/day. Further details on the site history and characteristics are described elsewhere (LeBlanc, 1984; LeBlanc et al., 1991; Repert et al., 2006).

Two regions of the aquifer were chosen for the field experiments, one in the Fe-reducing zone of the aquifer resulting from sewage contamination (located near well F625, see Fig. 3.1), and one in the pristine, oxic zone of the aquifer (located near well F168). In each area an array of multilevel samplers (MLS) exists that allows collection of breakthrough curves at several distances downgradient from an injection well. A summary of the background water chemistry at the injection wells used for the three field experiments are shown in Table 3.1.

#### 3.2 Field Experiment Methodology

Three tracer tests were performed at the field site in August 2006: (1) injection of CsI and NaBr into the oxic zone of the aquifer at F168-M17-02 (Oxic I<sup>-</sup>), (2) injection of CsBr and NaIO<sub>3</sub> into the oxic zone at F168-M17-08 (Oxic IO<sub>3</sub><sup>-</sup>), and (3) injection of CsBr and NaIO<sub>3</sub> into the Fe-reducing zone of the aquifer at F625-M02-09 (Anoxic IO<sub>3</sub><sup>-</sup>). A summary of the injections is shown in Table 3.2. For all three

tracer tests, groundwater was collected from wells in the same area (within 5-10 m) and depth interval as the injection wells. Tracer salts were added to the groundwater and mixed well before injecting. In order to prevent oxygen from entering the test performed in the Fe-reducing zone, the injection water was collected in a N<sub>2</sub> purged jet fuel bladder that was impervious to oxygen. The tracers were dissolved in a small amount of deionized water (boiled to remove oxygen) and pumped into the bladder, followed by several rinses with boiled, deionized water. However, some oxygen was inadvertently allowed into the bladder during the injection, resulting in low concentrations of dissolved oxygen in the injectate.

Groundwater samples were collected from downgradient MLS at various times and distances in order to create breakthrough curves. Using a peristaltic pump, each MLS port was purged with 150 mL of groundwater before collecting water samples for in-field (pH, conductivity) and laboratory analyses. Lab samples were filtered through a 0.45  $\mu$ m filter. Samples collected for iodine analysis were kept in the dark and refrigerated until they could be analyzed (within 4 hours) by spectrophotometer. Samples collected for Br and other anions were frozen. Br was measured using either ICP-MS (for samples containing I<sup>-</sup> or I<sub>2</sub>) or flow injection analysis (for samples containing only IO<sub>3</sub><sup>-</sup>). A subset of Br samples was analyzed by both methods in order to verify agreement between the two methods. Selected samples were also analyzed by ion chromatography for nitrate, phosphate, chloride, sulfate, and ammonium. Samples collected for elemental analysis by ICP-AES (Na, K, Mg, Ca, Mn, Fe, Si, P) and ICP-MS (Cs, Br) were acidified to pH 2 with trace metal grade nitric acid.

Iodine species were measured using a UV-Vis spectrophotometer on three separate samples as described in Section 2.1.6.

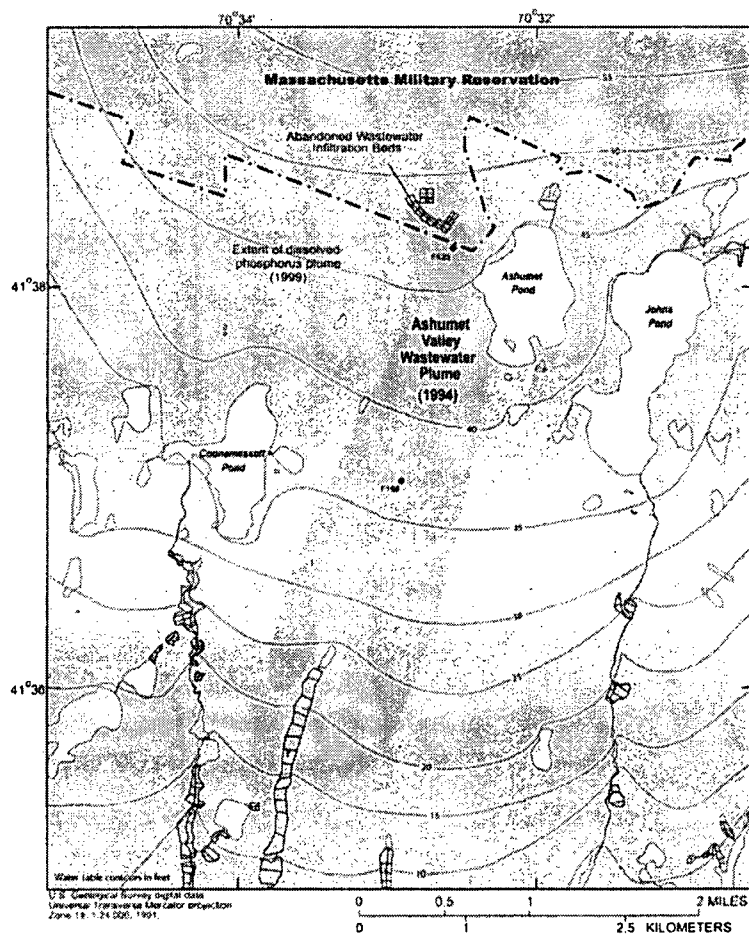


Figure 3.1. Map of the Cape Cod field site showing the extent of the wastewater plume and the locations of the two study areas (wells F625 and F168).

Table 3.1. Background Chemistry at Injection Wells Used In Field Experiments

Injection Well	DO	Ca	K	Mg	Na	Mn	Fe	
	mg/L	mol/L						
F168-M17-02	4.34	$9.22 \times 10^{-06}$	$1.31 \times 10^{-05}$	$2.94 \times 10^{-05}$	$2.43 \times 10^{-04}$	$5.32 \times 10^{-07}$	bdl	
F168-M17-08	7.45	$1.70 \times 10^{-05}$	$1.52 \times 10^{-05}$	$3.71 \times 10^{-05}$	$2.32 \times 10^{-04}$	$2.63 \times 10^{-07}$	bdl	
F625-M02-09	bdl	$1.98 \times 10^{-04}$	$8.45 \times 10^{-05}$	$5.91 \times 10^{-05}$	$8.99 \times 10^{-04}$	$2.59 \times 10^{-06}$	$2.07 \times 10^{-04}$	
	pH	Alk	P	Si	Cl	SO <sub>4</sub> <sup>2-</sup>	NH <sub>4</sub> <sup>+</sup>	
		meq/L	mol/L					
F168-M17-02	4.71	bdl	bdl	$1.12 \times 10^{-04}$	$2.54 \times 10^{-04}$	$2.12 \times 10^{-04}$	bdl	
F168-M17-08	5.06	0.005	bdl	$1.36 \times 10^{-04}$	$2.04 \times 10^{-04}$	$2.13 \times 10^{-04}$	bdl	
F625-M02-09	6.62	0.953	$9.67 \times 10^{-05}$	$2.25 \times 10^{-04}$	$4.94 \times 10^{-04}$	$1.44 \times 10^{-04}$	$5.83 \times 10^{-06}$	

**Table 3.2. Tracer Test Characteristics and Injected Tracer Concentrations**

	<i>Oxic I<sup>-</sup></i>	<i>Oxic IO<sub>3</sub><sup>-</sup></i>	<i>Anoxic IO<sub>3</sub><sup>-</sup></i>
Injection Port	F168 M17-02	F168 M17-08	F625 M02-09
Injection Altitude, m to sea level	8.21	6.75	1.02
Volume, L	362	383	179
Cs, mM	1.07	1.06	1.03
I, mM	1.13	1.05	0.98
Br, mM	1.13	1.02	1.01
Na, mM	1.26	1.26	2.50
pH	4.70	5.18	6.53

### 3.3 Results and Discussion

#### 3.3.1 Iodine Oxidation in the Oxidic Iodide Tracer Test

Results from the oxic I<sup>-</sup> injection demonstrated that iodide was oxidized to both I<sub>2</sub> and IO<sub>3</sub><sup>-</sup> during the course of the tracer test (Figure 3.2). Very little oxidation occurred over the first 1 m of transport, but after 2 m more than 20% of the injected I<sup>-</sup> had been oxidized, primarily to I<sub>2</sub>, and after 4 m even more oxidation had occurred. This region of the aquifer was characterized by oxygenated groundwater (4.0-5.8 mg/L dissolved O<sub>2</sub>) and low pH (4.5-5.1), creating conditions conducive for the oxidation of iodide. There are several possible oxidants that may be responsible for iodide oxidation, including dissolved O<sub>2</sub>, NO<sub>3</sub><sup>-</sup>, and mineral phases such as Mn and Fe oxides (Fig. 1.1). Mn oxides are clearly the most likely oxidant, however, because oxygen is slow to react with iodide and nitrate concentrations were extremely low (<1 μM).

Manganese oxides have been shown to abiotically oxidize a variety of inorganic contaminants such as As(III) and Cr(III) and are likely oxidants of I<sup>-</sup> as well (Fendorf and Zasoski, 1992; Scott and Morgan, 1995; Anschutz et al., 2000; Truesdale et al., 2001; Manning et al., 2002). Amirbahman et al. (2006) found that sediments collected from the same tracer test region oxidized As(III) to As(V) in laboratory batch experiments, most likely caused by Mn-oxides. Sediment samples collected closest to the tracer test location

(F168-15) contained 2.04 μmol/g reductively extractable Mn (Amirbahman et al., 2006). If we consider an estimated bulk density of 4000 g/L in the field, then there was an excess of Mn-oxide available for I<sup>-</sup> oxidation (8.16 mM Mn). As shown in Figure 3.2, there was an increase in the concentration of dissolved Mn during this tracer test, arriving just after the Br breakthrough curve, thus providing evidence that Mn oxides were the likely electron acceptor responsible for I<sup>-</sup> oxidation. The observed dissolved Mn concentrations increased with transport distance from the injection well, reaching up to 7.6 x 10<sup>-5</sup> M at 2 m downgradient. Mn<sup>2+</sup> is known to adsorb to mineral surfaces, thus the observed dissolved Mn should be only a fraction of the total amount of Mn<sup>2+</sup> produced during the reaction of Mn oxides with I<sup>-</sup>. An increase in Mn concentrations was not observed in the oxic tracer test in which IO<sub>3</sub><sup>-</sup> was injected, and thus the increase in Mn concentrations cannot be attributed to ion exchange reactions releasing sorbed Mn<sup>2+</sup>. The mass balance for I indicates that little methyl-I was formed in the experiments.

#### 3.3.2 Iodate Adsorption in the Oxidic Iodate Tracer Test

Iodate was significantly retarded relative to the Br tracer (Figure 3.3) when iodate was injected into an oxic region of the aquifer. After 4 m of transport, the IO<sub>3</sub><sup>-</sup> pulse became very spread out, and reached a maximum of 29% of the injection concentration. The retardation and significant tailing indicates that iodate adsorbs to the

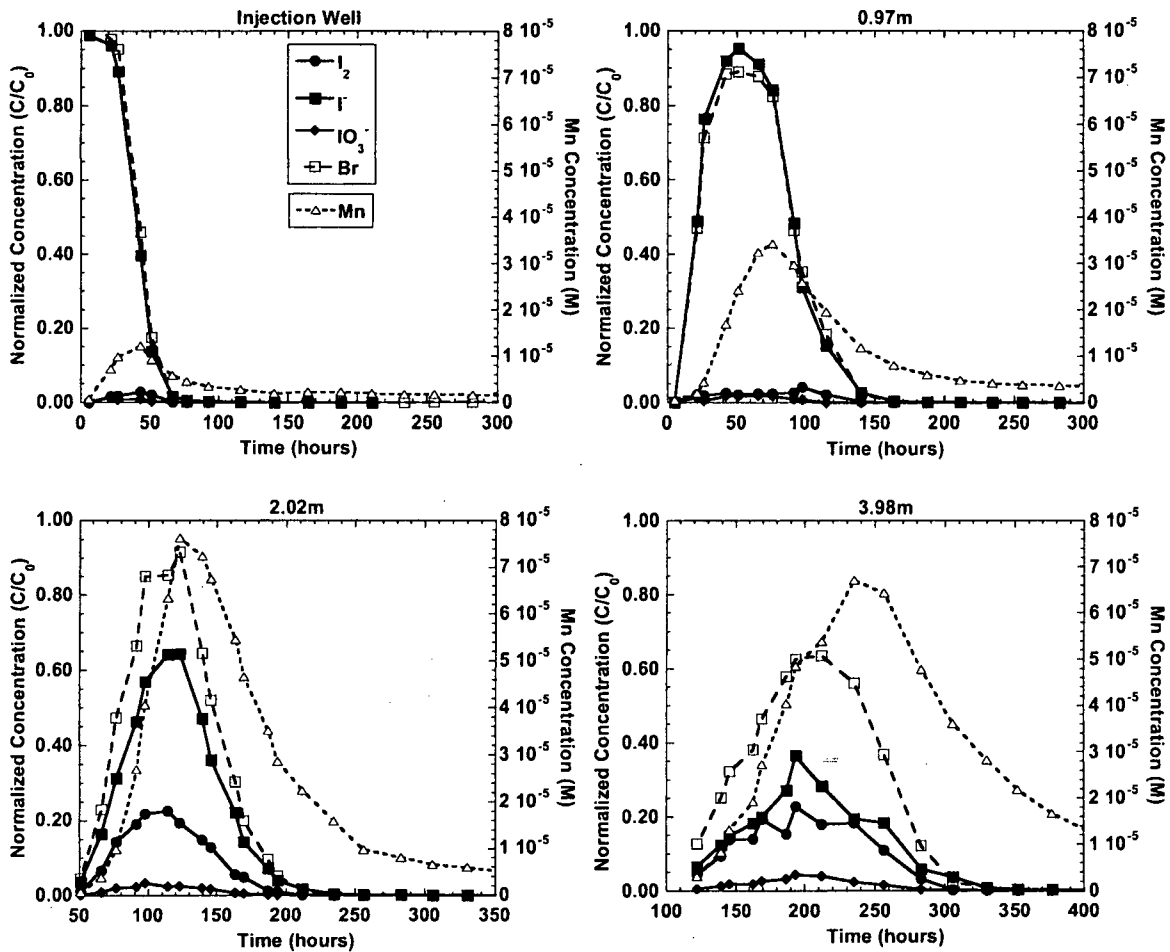


**Figure 3.2. Breakthrough curves showing  $\text{Br}^-$ ,  $\text{I}^-$ ,  $\text{I}_2$ ,  $\text{IO}_3^-$ , and Mn concentrations at various distances downgradient of the injection well in the oxic  $\text{I}^-$  tracer test. All Br and I species concentrations are normalized to the injection concentration.**

sediments under these conditions. Other researchers have observed that iodate exhibits higher sorption and is more retarded than iodide (Couture and Seitz, 1983; Hu et al., 2005). Hu et al. (2005) observed both iodate sorption and reduction to  $\text{I}^-$  during batch and column studies with a variety of soils and clay minerals. They postulated that structural  $\text{Fe(II)}$  present in the mineral phases was responsible for the iodate reduction. In our study, however, no iodide was detected during the tracer test. Nevertheless, iodate exhibited non-conservative transport in this experiment.

### 3.3.3 Iodate Reduction in the Anoxic Iodate Tracer Test

Iodate was injected into an iron-reducing region of the aquifer located near well F625. The iodate was quickly reduced to iodide, with more than 50% reduced after only 1 m of transport (Figure 3.4). Transport of iodine was conservative, matching Br transport very closely. No  $\text{I}_2$  was detected during the tracer test, suggesting that iodate was reduced directly to iodide. This is in contrast to the oxidation of iodide, which proceeded through  $\text{I}_2$  to  $\text{IO}_3^-$ . It is unclear by what mechanism iodate reduction occurs in this system. A number of inorganic compounds have been shown or proposed to be

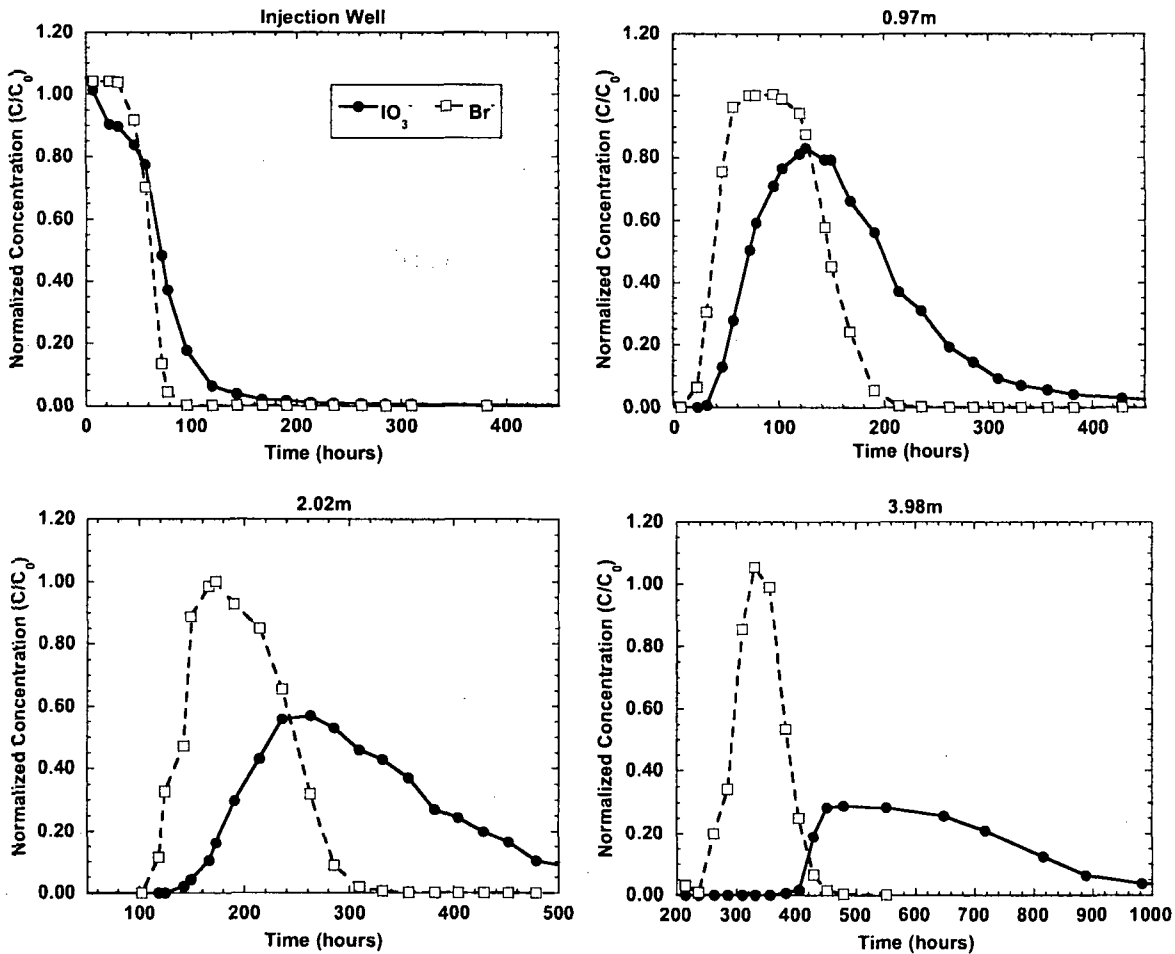


**Figure 3.3. Iodate and Br breakthrough curves at various distances downgradient from the injection well in the oxidic iodate tracer test. All concentrations are normalized to the injection concentration. Note the different time scales for different wells.**

reductants of iodate, including Fe<sup>2+</sup> (both dissolved and solid phases), dissolved Mn<sup>2+</sup>, and dissolved S<sup>2-</sup> (Councell et al., 1997; Anschutz et al., 2000; Hu et al., 2005). Microbially mediated reduction by *Desulfovibrio desulfuricans* and *Shewanella putrefaciens* has been demonstrated (Councell et al., 1997; Farrenkopf et al., 1997). During this tracer test, there was a decrease in the concentrations of dissolved Fe that coincided with the I pulse, however, this may have been due to the fact that some dissolved oxygen contaminated the injectate solution, possibly causing oxidation of Fe(II) and subsequent precipitation of Fe(III).

### 3.3.4 Cesium Retardation and Attenuation

Cesium was significantly retarded relative to the conservative tracer (Br) in both tracer tests performed in the oxidic zone of the aquifer near F168 (Figures 3.5 and 3.6). Cs is so attenuated that after only 4 m, the maximum Cs concentration reached was only 5% of the injected concentration. A pulse of dissolved K was liberated from the aquifer sediments during the tracer tests, an indicator that Cs uptake in the tracer tests was due to cation exchange. Cation exchange processes are generally considered to be independent of pH, and while this is generally true for Cs over a wide range of conditions,

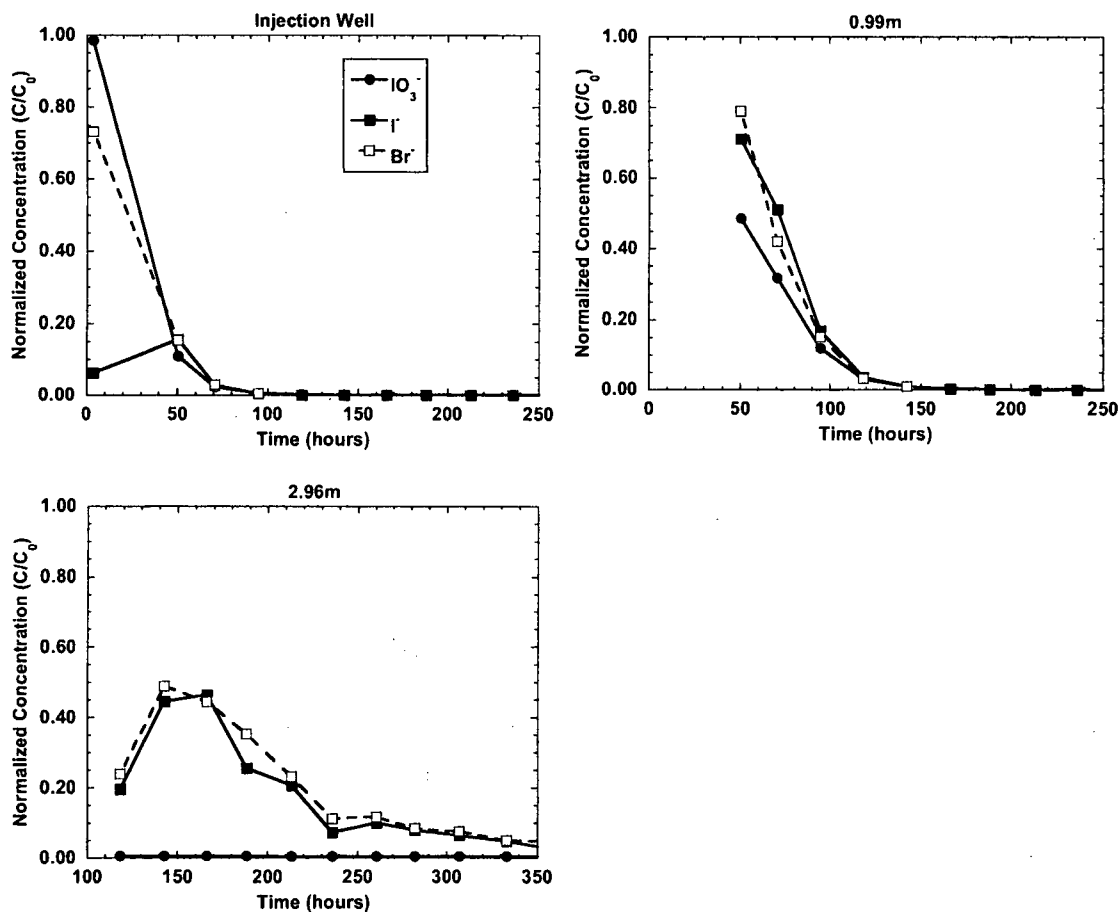


Figure 3.4.  $\text{Br}^-$ ,  $\text{IO}_3^-$  and  $\text{I}^-$  breakthrough curves at various distances downgradient from the injection well for the anoxic iodate injection. Concentrations are normalized to the injection concentrations.

Poinssot et al. (1999) found Cs sorption to exhibit pH dependence (sorption increased with increasing pH for the pH range 3-6) at low ionic strength (in 0.01M  $\text{NaClO}_4$  solution). Because the oxic zone of the Cape Cod aquifer has a low ionic strength (Table 3.2), it is possible that the pH difference between the two tracer tests (5.18 at M17-08 vs 4.70 at M17-02) affected Cs sorption. Reactive transport modeling of the data is necessary to determine if there was a real difference in Cs sorption between the two oxic tracer tests. The disappearance of Cs from the injection well during the anoxic tracer test is shown in Figure 3.7. Cs and Br disappearance appeared to be qualitatively similar in this tracer test to the behavior observed in the oxic tests (Figure 3.6).

### 3.4 Summary of Field Experiments

This study demonstrated that both iodine and cesium may behave non-conservatively in groundwater systems. In the oxic zone of the aquifer, iodide was oxidized to  $\text{I}_2$  and  $\text{IO}_3^-$ , and  $\text{IO}_3^-$  transport was retarded. Iodide was most likely oxidized by Mn oxides present in the aquifer sediments. In the iron-reducing zone of the Cape Cod sand and gravel aquifer,  $\text{IO}_3^-$  was reduced to  $\text{I}^-$ . Cs was even more retarded than  $\text{IO}_3^-$  in both the oxic and reducing zones of the aquifer, due to cation exchange with K. These results demonstrate the importance of taking redox transformations into consideration when predicting iodine transport in the field.

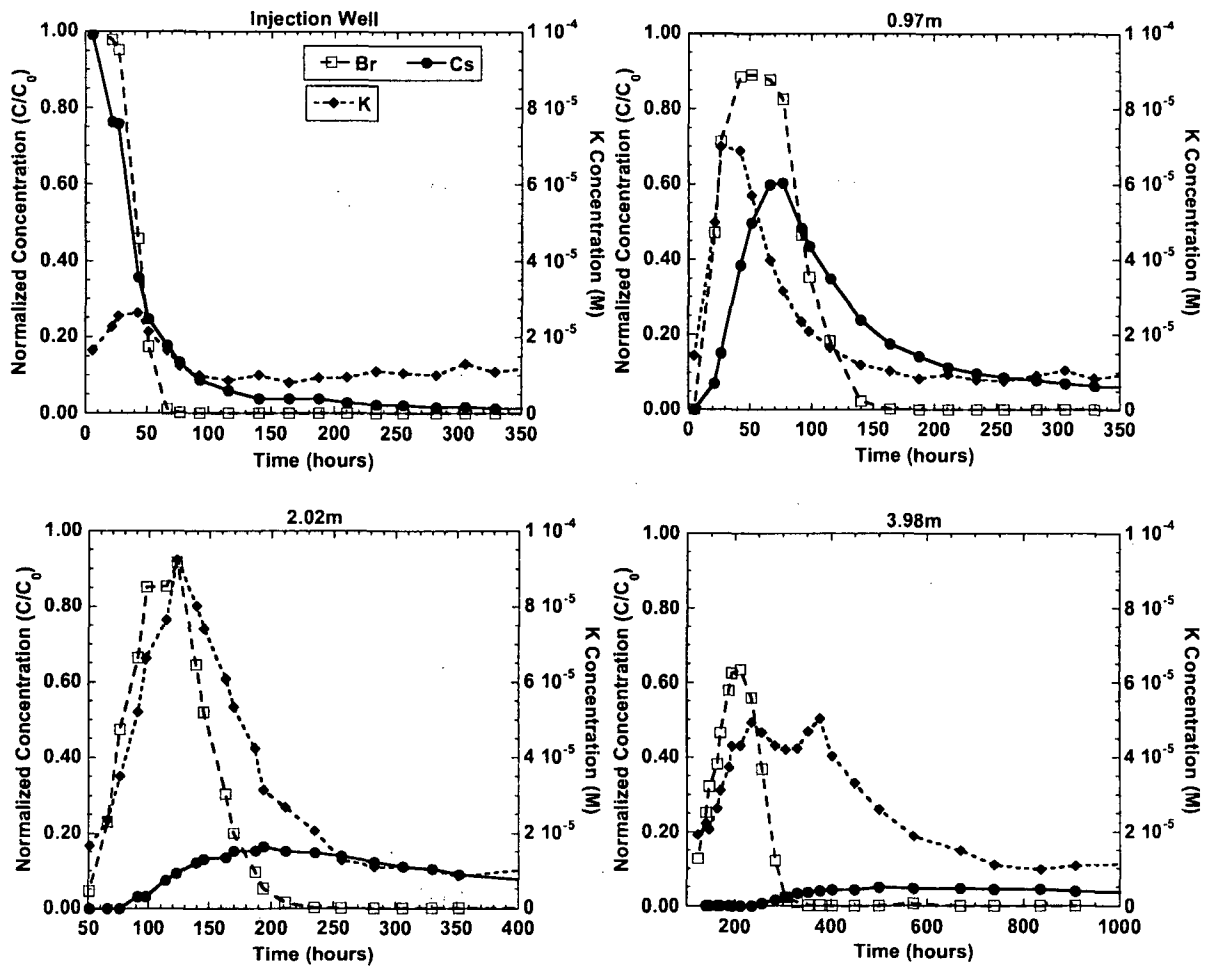


Figure 3.5. Cs, Br, and K breakthrough curves at various distances downgradient from the injection well in the oxic iodide tracer test (well F168-M17-02). Cs and Br concentrations are normalized to the concentrations in the injectate. Note the different time scales in each panel.

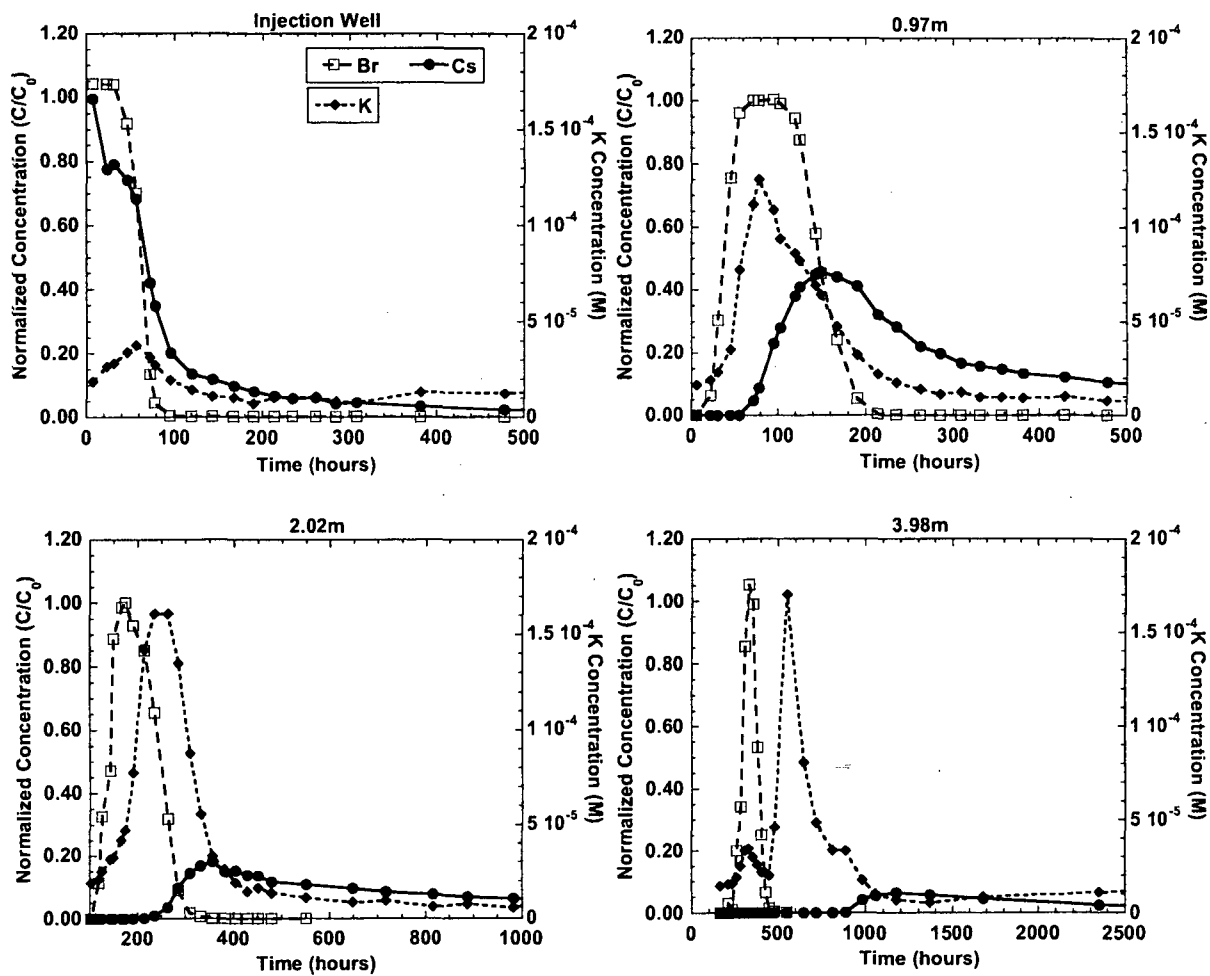


Figure 3.6. Cs, Br, and K breakthrough curves at various distances downgradient from the injection well in oxidic iodate tracer test (well F168-M17-08). Cs and Br concentrations are normalized to the concentrations in the injectate. Note the different time scales in each panel.



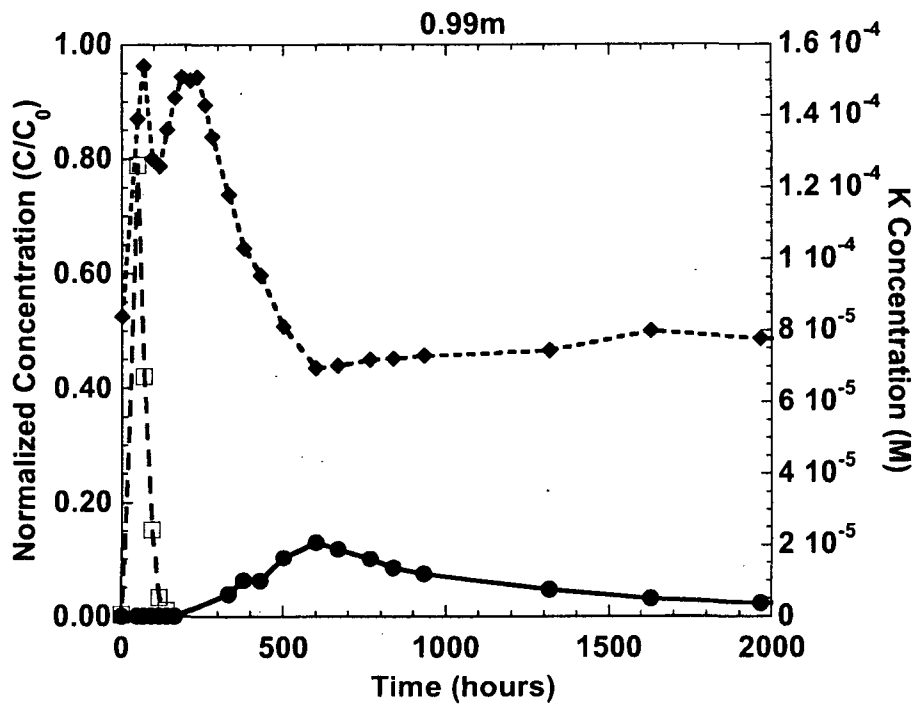
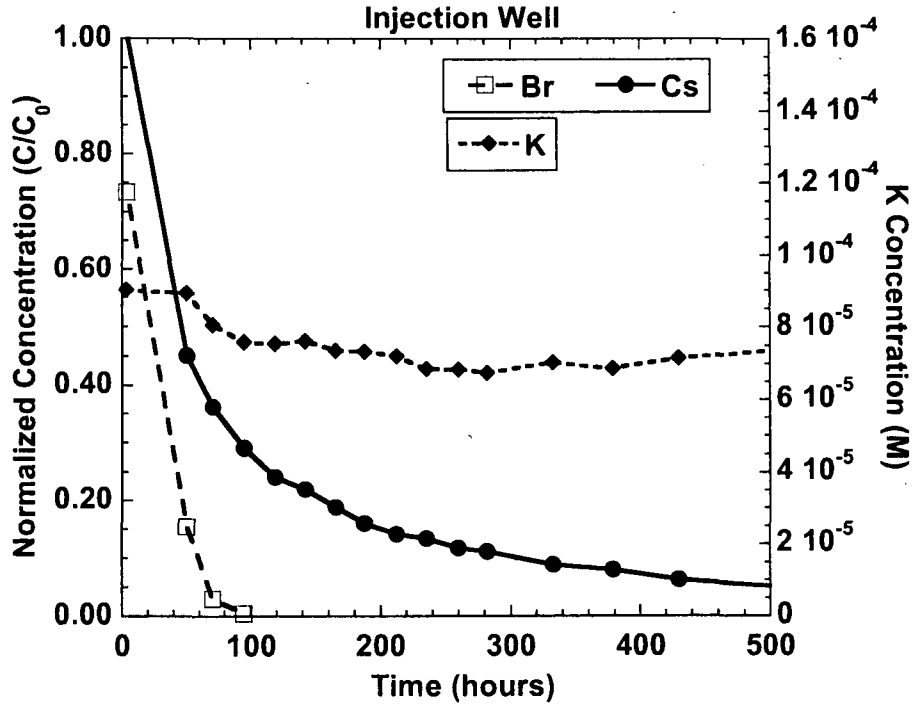
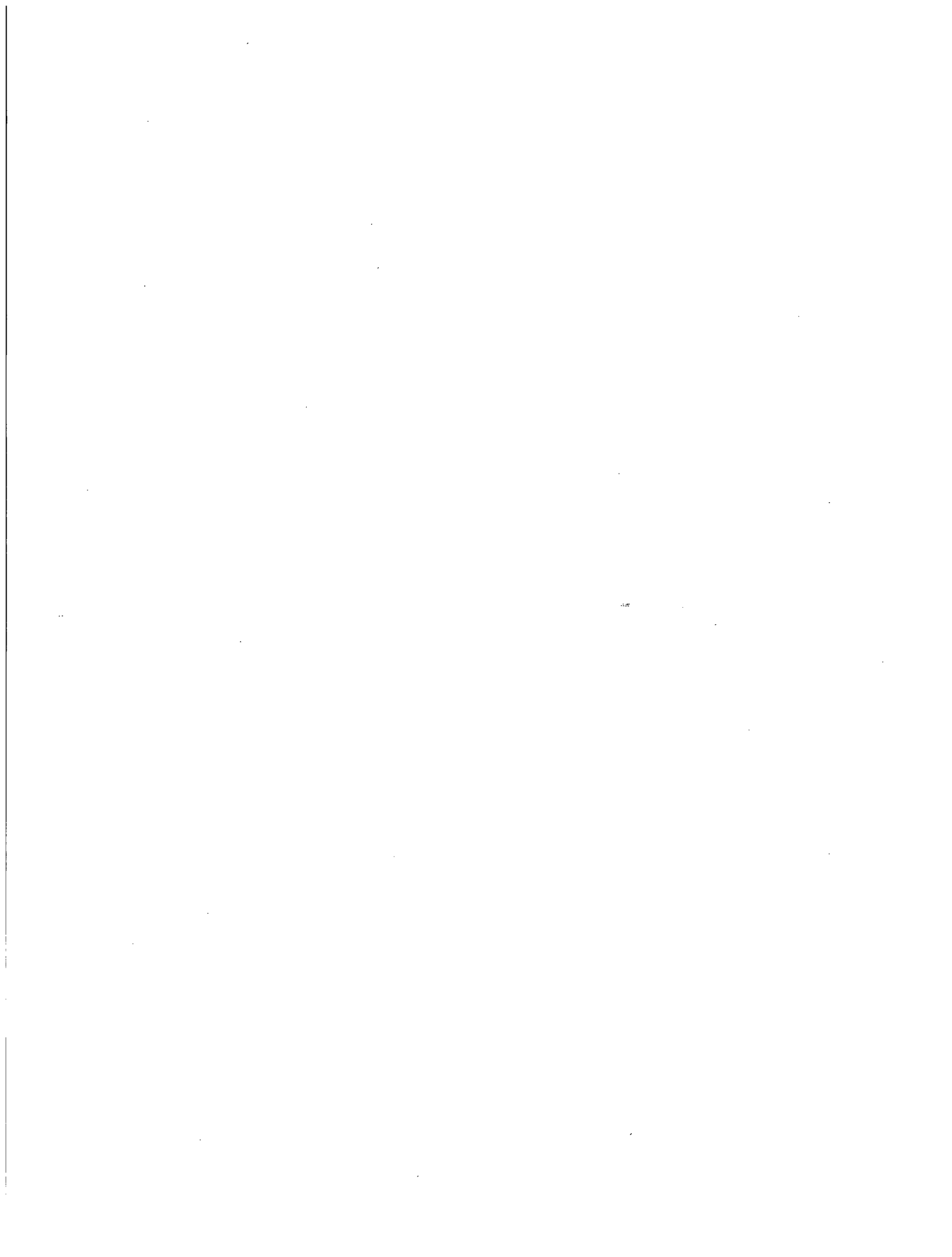


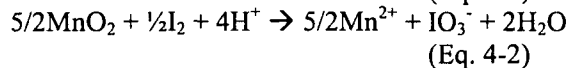
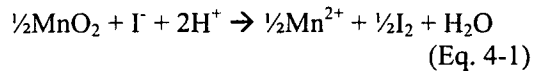
Figure 3.7. Cs, Br, and K during the anoxic iodate tracer test (well F625-M12-09). No Cs was detected beyond 0.99 m downgradient. Cs and Br concentrations are normalized to the concentrations in the injectate.



## 4 SUMMARY

Radioactive isotopes of Cs ( $^{137}\text{Cs}$ ) and I ( $^{131}\text{I}$  and  $^{129}\text{I}$ ) are produced during nuclear fission and have been released into the environment through nuclear fallout from weapons tests and nuclear accidents such as Chernobyl. Scientists and regulators need information on the geochemical behavior of Cs and I in order to accurately predict their behavior in subsurface environments. Prior to this study, very little information on the redox reactions of iodine in the subsurface was available. Cs sorption and transport has been extensively studied in laboratory batch and column experiments, but very little information on field studies in saturated environments is available. In this study iodide oxidation, sorption of I species, and sorption of Cs species were investigated through a combination of laboratory and field experiments.

Through the use of batch kinetic experiments, we discovered that the manganese oxide, birnessite, could oxidize iodide ( $\text{I}^-$ ) to elemental iodine ( $\text{I}_2$ ) and iodate ( $\text{IO}_3^-$ ) in a two-step process, according to the following reactions:



The oxidation kinetics depend on a variety of factors including ionic strength, pH, and birnessite concentration. Both  $\text{I}_2$  and to a lesser extent  $\text{IO}_3^-$  adsorb to birnessite, reaching concentrations of up to 0.25 and 0.024 mmol/g, respectively.  $\text{I}^-$  may also adsorb to birnessite, but this probably occurs quickly relative to the oxidation of  $\text{I}^-$  to  $\text{I}_2$ . Reaction 4-1 appears to be first order with respect to initial  $\text{I}^-$  concentration,  $\text{H}^+$  concentration, and birnessite concentration, with pseudo-first order rate constants ranging from 0.064 to 5.30  $\text{hr}^{-1}$ . Reaction 4-2, however, does not appear to be strictly first order with respect to initial  $\text{I}_2$  concentration and may be complicated by  $\text{I}_2$  sorption. Despite this fact, a simple model which considers both Reaction 4-1

and 4-2 to be first order with respect to I fits the data fairly well.

In batch sediment experiments, uptake of  $\text{I}^-$  was low (2-3% at an initial concentration of 1 mM). In binary sediment-birnessite experiments,  $\text{I}^-$  was oxidized to  $\text{I}_2$  and  $\text{IO}_3^-$ . In a 1-m long column filled with aquifer sediment,  $\text{I}^-$  uptake was low at pH 4.8, but increased when the pH was lowered to 4.50. At pH 4.5,  $\text{I}^-$  concentrations increased during breakthrough to 90% of the input concentration, then slowly increased to 93% over the next few days. No  $\text{I}_2$  or  $\text{IO}_3^-$  was detected during the column experiments, suggesting that  $\text{I}^-$  was oxidized to elemental  $\text{I}_2$ , which was volatilized from the samples prior to analysis. During a field tracer test in which 1 mM  $\text{I}^-$  was injected into the oxic zone of a sand and gravel aquifer on Cape Cod, MA,  $\text{I}^-$  was oxidized to  $\text{I}_2$  (up to 46%) and  $\text{IO}_3^-$  (up to 6%) during 4 m of transport. Mn-oxides appeared to be responsible for the  $\text{I}^-$  oxidation, as evidenced by a pulse of dissolved Mn that was released from the sediments during the experiment. The tracer tests allowed us to investigate iodide oxidation over much larger transport distances than is feasible in the laboratory. Over 1 m of transport,  $\text{I}^-$  behaved similarly in the column experiment and tracer test, although low concentrations of  $\text{I}_2$  and  $\text{IO}_3^-$  (1-2% of the input concentration) were measured in the tracer test.

Iodate sorption to aquifer sediments was higher than iodide, with up to 12% of the initial concentration (1 mM) taken up by sediments in batch experiments. In a tracer test in which 1 mM  $\text{IO}_3^-$  was injected into the oxic zone of the aquifer,  $\text{IO}_3^-$  was retarded relative to bromide. After 4 m of transport, the  $\text{IO}_3^-$  pulse became very spread out and reached a maximum of 29% of the injection concentration. No evidence of reduction of  $\text{IO}_3^-$  in either the batch experiments or the oxic tracer test was found. However, when  $\text{IO}_3^-$  was injected into the Fe-reducing zone of the aquifer, it was completely reduced to  $\text{I}^-$  during 3 m of transport. A number of abiotic and biotic pathways for  $\text{IO}_3^-$  reduction are

possible, including reduction by  $\text{Fe}^{2+}$  or  $\text{Mn}^{2+}$ , and microbially mediated reduction.

In batch experiments with aquifer sediment, up to 22% of the Cs (initial concentration of 0.5 mM) was sorbed. During the tracer tests, Cs sorption was strong, with the breakthrough very attenuated. After 4 m of transport the Cs concentration peaked at only 5% of the injection concentration (1 mM). Following the long peak in Cs concentration, a very long tail of low Cs concentrations continued for several months.

The Cs appeared to adsorb via cation exchange, as evidenced by a pulse of K released from the sediments during the tracer tests.

While the Cs and I concentrations used in these experiments are much higher than would be relevant for concentrations of radioactive isotopes of these elements, the studies are relevant for revealing reaction mechanisms that affect the transport of the radionuclides in the environment.

## 5 REFERENCES

- Ainsworth C. C., Zachara J. M., Wagnon K., McKinley S., Liu C., Smith S. C., Schaef H. T. and Gassman P. L. (2005) Impact of highly basic solutions on sorption of Cs<sup>+</sup> to subsurface sediments from the Hanford site, USA, *Geochim. Cosmochim. Acta* **69**, 4787-4800.
- Amirbahman A., Kent D. B., Curtis G. P. and Davis J. A. (2006) Kinetics of sorption and abiotic oxidation of arsenic(III) by aquifer materials, *Geochim. Cosmochim. Acta* **70**, 533-547.
- Anschutz P., Sundby B., Lefrancois L., Luther III, George W. and Mucci A. (2000) Interactions between metal oxides and species of nitrogen and iodine in bioturbated marine sediments, *Geochim. Cosmochim. Acta* **64**, 2751-2763.
- APHA. (1992) Standard methods for the examination of water and wastewater, 18<sup>th</sup> Edition.
- Blagoeva R. and Zikovskiy L. (1995) Geographic and vertical distribution of Cs-137 in soils in Canada, *J. Environ. Radioactivity* **27**, 269-274.
- Comans R. N. J., Haller M. and de Preter P. (1991) Sorption of cesium on illite: Non-equilibrium behaviour and reversibility, *Geochim. Cosmochim. Acta* **55**, 433-440.
- Coston, J.A., Fuller, C.C., and Davis, J.A. (1995) Pb<sup>2+</sup> and Zn<sup>2+</sup> adsorption by a natural Al- and Fe-bearing surface coating on an aquifer sand, *Geochimica et Cosmochimica Acta*, **59**, 3535-3548.
- Councell T. B., Landa E. R. and Lovley D. R. (1997) Microbial reduction of iodate, *Water Air Soil Poll.* **100**, 99-106.
- Couture R. A. and Seitz M. G. (1983) Sorption of anions of iodine by iron oxides and kaolinite, *Nucl. Chem. Waste Manag.* **4**, 301-306.
- Davis, J.A., Kent, D.B., Coston, J.A., Hess, K.M., and Joye, J.L. (2000) Multispecies reactive tracer test in an aquifer with spatially variable chemical conditions, *Water Resources Research*, **36**, 119-134.
- Farrenkopf A. M., Dollhopf M. E., Chadhain S. N., Luther III, George W. and Nealson K. H. (1997) Reduction of iodate in seawater during Arabian Sea shipboard incubations and in laboratory cultures of the marine bacterium *Shewanella putrefaciens* strain MR-4, *Mar. Chem.* **57**, 347-354.
- Fendorf S. E. and Zasoski R. J. (1992) Chromium(III) oxidation by  $\alpha$ -MnO<sub>2</sub>. 1. Characterization, *Environ. Sci. Technol.* **26**, 79-85.
- Filipovic-Vincekovic N., Barisic D., Masic N. and Lulic S. (1991) Distribution of fallout radionuclides through soil surface layer, *J. Radioanal. Nucl. Chem. Art.* **148**, 53-62.
- Fuhrmann M., Bajt S. and Schoonen M. A. A. (1998) Sorption of iodine on minerals investigated by X-ray absorption near edge structure (XANES) and <sup>125</sup>I tracer sorption experiments, *Appl. Geochem.* **13**, 127-141.
- Fuller, C.C., Davis, J.A., Coston, J.A. and Dixon, E. (1996) Characterization of metal adsorption heterogeneity in a sand and gravel aquifer, Cape Cod, Massachusetts, *J. Contam. Hydrology*, **22**, 165-187.

- Hem J. D., Roberson C. E. and Fournier R. B. (1982) Stability of  $\beta$ -MnOOH and manganese oxide deposition from springwater, *Water Resources Research* **18**, 563-570.
- Hu Q., Zhao P., Moran J. E. and Seaman J. C. (2005) Sorption and transport of iodine species in sediments from the Savannah River and Hanford Sites, *J. Contam. Hydrol.* **78**, 185-205.
- Kaplan D. I., Serne J., Parker K. E. and Kutnyakov I. V. (2000) Iodide sorption to subsurface sediments and illitic minerals, *Environ. Sci. Technol.* **34**, 399-405.
- Kent D. B., Davis J. A., Anderson L. C. D., Rea B. A. and Waite T. D. (1994) Transport of chromium and selenium in the suboxic zone of a shallow aquifer: Influence of redox and adsorption reactions, *Water Resources Research* **30**, 1099-1114.
- Krumhansl J. L., Brady P. V. and Anderson H. L. (2001) Reactive barriers for  $^{137}\text{Cs}$  retention, *J. Contam. Hydrol.* **47**, 233-240.
- LeBlanc D. R. (1984) Sewage plume in a sand and gravel aquifer, Cape Cod, Massachusetts, *U. S. Geol. Surv. Water Supply Pap.* **2218**, 28.
- LeBlanc D. R., Garabedian S. P., Hess K. M., Gelhar L. W., Quadri R. D., Stollenwerk K. G. and Wood W. W. (1991) Large-scale natural-gradient tracer test in sand and gravel aquifer, Cape Cod, Massachusetts, 1, Experimental design and observed tracer movement, *Water Resources Research* **27**, 895-910.
- Luther III G. W., Ferdelman T., Culberson C. H., Kostka J. and Wu J. (1991) Iodine chemistry in the water column of the Chesapeake Bay: Evidence for organic iodine forms, *Est. Coastal Shelf Sci.* **32**, 267-279.
- Manning B. A., Fendorf S. E., Bostick B. and Suarez D. D. (2002) Arsenic(III) oxidation and arsenic(V) adsorption reactions on synthetic birnessite, *Environ. Sci. Technol.* **36**, 976-981.
- McKenzie R. M. (1981) The surface charge on manganese dioxides, *Aust. J. Soil Res.* **19**, 41-50.
- McKenzie R. M. (1971) The synthesis of birnessite, cryptomelane, and some other oxides and hydroxides of manganese, *Mineral. Mag.* **38**, 493-502.
- Oktay S. D., Santschi P. H., Moran J. E. and Sharma P. (2001)  $^{129}\text{I}$  and  $^{127}\text{I}$  transport in the Mississippi River, *Environ. Sci. Technol.* **35**, 4470-4476.
- Oktay S. D., Santschi P. H., Moran J. E. and Sharma P. (2000) The  $^{129}\text{I}$  iodine bomb pulse recorded in Mississippi River Delta sediments: Results from isotopes of I, Pu, Cs, Pb, and C, *Geochim. Cosmochim. Acta* **64**, 989-996.
- Poinssot C., Baeyens B. and Bradbury M. H. (1999) Experimental and modeling studies of caesium sorption on illite, *Geochim. Cosmochim. Acta* **63**, 3217-3227.
- Rao U. and Fehn U. (1999) Sources and reservoirs of anthropogenic iodine-129 in western New York, *Geochim. Cosmochim. Acta* **63**, 1927-1938.

- Reithmeier H., Lazarev V., Ruhm W., Schwikowski M., Gaggeler H. W. and Nolte E. (2006) Estimate of european  $^{129}\text{I}$  releases supported by  $^{129}\text{I}$  analysis in an alpine ice core, *Environ. Sci. Technol.* **40**, 5891-5896.
- Repert D. A., Barber L. B., Hess K. M., Keefe S. H., Kent D. B., LeBlanc D. R. and Smith R. L. (2006) Long-term natural attenuation of carbon and nitrogen within a groundwater plume after removal of the treated wastewater source, *Environ. Sci. Technol.* **40**, 1154-1162.
- Schlegel M. L., Reiller P., Mercier-Bion F., Barre N. and Moulin V. (2006) Molecular environment of iodine in naturally iodinated humic substances: Insight from X-ray absorption spectroscopy, *Geochim. Cosmochim. Acta* **70**, 5536-5551.
- Schwehr K., Santschi P. H. and Elmore D. (2005) The dissolved organic iodine species of the isotopic ratio of  $^{129}\text{I}/^{127}\text{I}$ : A novel tool for tracing terrestrial organic carbon in the estuarine surface waters of Galveston Bay, Texas, *Limnol. Oceanogr. Methods* **3**, 326-337.
- Scott M. J. and Morgan J. J. (1995) Reactions at oxide surfaces. 1. Oxidation of As(III) by synthetic birnessite, *Environ. Sci. Technol.* **29**, 1898-1905.
- Sheppard M. I., Thibault D. H., McMurry J. and Smith P. A. (1995) Factors affecting the soil sorption of iodine. *Water Air Soil Poll.* **83**, 51-67.
- Truesdale V. W. (1978) The automatic determination of iodate- and total-iodine in seawater, *Mar. Chem.* **6**, 253-273.
- Truesdale V. W., Watts S. F. and Rendell A. R. (2001) On the possibility of iodide oxidation in the near-surface of the Black Sea and its implications to iodine in the general ocean, *Deep-Sea Research I* **48**, 2397-2412.
- Warner J. A., Casey W. H. and Dahlgren R. A. (2000) Interaction kinetics of  $\text{I}_2(\text{aq})$  with substituted phenols and humic substances, *Environ. Sci. Technol.* **34**, 3180-3185.
- Yamaguchi N., Nakano M., Tanida H., Fujiwara H. and Kihou N. (2006) Redox reaction of iodine in paddy soil investigated by field observation and the I K-edge XANES fingerprinting method, *J. Environ. Radioactivity* **86**, 212-226.
- Yu Z., Warner J. A., Dahlgren R. A. and Casey W. H. (1996) Reactivity of iodide in volcanic soils and noncrystalline soil constituents, *Geochim. Cosmochim. Acta* **60**, 4945-4956.
- Zachara J. M., Smith S. C., Liu C., McKinley J. P., Serne R. J. and Gassman P. L. (2002) Sorption of  $\text{Cs}^+$  to micaceous subsurface sediments from the Hanford site, USA, *Geochim. Cosmochim. Acta* **66**, 193-211.





<b>NRC FORM 335</b> (9-2004) NRCMD 3.7		<b>U.S. NUCLEAR REGULATORY COMMISSION</b>		<b>1. REPORT NUMBER</b> (Assigned by NRC, Add Vol., Supp., Rev., and Addendum Numbers, if any.)  NUREG/CR-6977	
<b>BIBLIOGRAPHIC DATA SHEET</b> (See instructions on the reverse)					
<b>2. TITLE AND SUBTITLE</b>  Redox and Sorption Reactions of Iodine and Cesium During Transport through Aquifer Sediments			<b>3. DATE REPORT PUBLISHED</b>		
			MONTH March	YEAR 2009	
<b>5. AUTHOR(S)</b>  James A. Davis and P. M. Fox			<b>4. FIN OR GRANT NUMBER</b>  Y6462		
			<b>6. TYPE OF REPORT</b>  Technical		
<b>8. PERFORMING ORGANIZATION - NAME AND ADDRESS</b> (If NRC, provide Division, Office or Region, U.S. Nuclear Regulatory Commission, and mailing address; if contractor, provide name and mailing address.)  U.S. Geological Survey 345 Middlefield Rd MS 465 Menlo Park, CA 94025			<b>7. PERIOD COVERED</b> (Inclusive Dates)  July 2006 - January 2008		
			<b>9. SPONSORING ORGANIZATION - NAME AND ADDRESS</b> (If NRC, type "Same as above"; if contractor, provide NRC Division, Office or Region, U.S. Nuclear Regulatory Commission, and mailing address.)  Division of Risk Analysis Office of Nuclear Regulatory Research U.S. Nuclear Regulatory Commission Washington DC 20555-0001		
<b>10. SUPPLEMENTARY NOTES</b> Mark Fuhrmann, NRC Project Manager					
<b>11. ABSTRACT</b> (200 words or less)  In order to further our understanding of the chemical behavior of I and Cs in groundwater systems, a series of laboratory and field experiments were undertaken. In order to determine Cs and I sorption and I oxidation, batch experiments with aquifer sediments and with binary sediment-Mn oxide systems were performed. Iodide transport was studied in a column filled with aquifer sediments. Three field tracer test experiments were performed to elucidate the redox chemistry and transport of I and Cs in an aquifer characterized by distinct geochemical zones: (1) injection of CsI into a well oxygenated zone of the aquifer, (2) injection of CsIO <sub>3</sub> into a well oxygenated zone, and (3) injection of CsIO <sub>3</sub> into a zone of the aquifer characterized by active Fe(III) reduction (but not sulfate reduction). The results of these experiments demonstrate that not only can redox transformations of iodine easily occur in groundwater systems, but also that I <sub>2</sub> and IO <sub>3</sub> behave non-conservatively by adsorbing to sediments and minerals. The results indicate the importance of considering the complex redox and sorption chemistry of iodine when predicting its transport in waste plumes.					
<b>12. KEY WORDS/DESCRIPTORS</b> (List words or phrases that will assist researchers in locating the report.)  cesium iodine iodate iodide adsorption contaminant transport redox field experiments				<b>13. AVAILABILITY STATEMENT</b> unlimited	
				<b>14. SECURITY CLASSIFICATION</b> (This Page) unclassified	
				(This Report) unclassified	
				<b>15. NUMBER OF PAGES</b> ...	
				<b>16. PRICE</b>	



Federal Recycling Program





UNITED STATES  
NUCLEAR REGULATORY COMMISSION  
WASHINGTON, DC 20555-0001

-----  
OFFICIAL BUSINESS